SPATIOTEMPORAL PATTERNS AND DRIVERS OF VEGETATION PHENOLOGY IN THE THREE-NORTH SHELTER FOREST PROGRAM REGION BASED ON SOLAR-INDUCED CHLOROPHYLL FLUORESCENCE

XU, A. Q.[1] – WANG, B. [1,2*] – WANG, Z. H.[1] – ZHANG, X.[1,2] – ZHANG, Q. L.[1,2]

[1]*Forestry College, Inner Mongolia Agricultural University, Hohhot 010019, China*

[2]*Forest Ecosystem National Observation and Research Station of Greater Khingan Mountains in Inner Mongolia, Genhe 022350, China*

[*]*Corresponding author*
e-mail: wbingbing2008@126.com

(Received 14th Jan 2025; accepted 19th Mar 2025)

Abstract. As an important ecological security barrier in China, studying the vegetation phenology in Three-North Shelter Forest Program (TNSFP) region is of great significance for monitoring the photosynthesis and carbon-water cycle of vegetation in northern terrestrial ecosystems under the background of global climate change. Based on the data of solar-induced chlorophyll fluorescence (SIF) from 2001 to 2023, the dynamic threshold method was used to extract the start time (SOS), the end time (EOS) and the length of growing season (LOS) of vegetation in the TNSFP region. Combined with linear trend analysis, the coefficient of variation (CV), the Hurst index (H), optimal parameter geographic detector, Pearson correlation analysis and other methods, the spatial-temporal variation characteristics and future trends of vegetation photosynthetic phenology in the TNSFP region were explored, and the driving force of spatial heterogeneity and temporal variations were analyzed. The results show that: (1) The spatial distribution of the SOS, EOS, and LOS in the western and southern parts of the study area showed early-late-long characteristics, respectively, while the eastern and northern parts showed late-early-short characteristics. (2) The SOS advanced at a rate of 0.16 d/a, the EOS delayed at a rate of 0.20 d/a, and the LOS extended at a rate of 0.26 d/a. (3) The SOS, EOS, and LOS in 23 years exhibited low fluctuation, and most areas will show a trend of delay, advanced, and shortening in the future. (4) In terms of spatial heterogeneity, elevation and precipitation are the dominant factors for the SOS, minimum temperature and maximum temperature are the dominant factors of the EOS, precipitation is the dominant factor of the LOS, and the interaction of each driving factor improves the explanatory power of spatial heterogeneity in vegetation photosynthetic phenology. (5) In terms of temporal variation, the correlations between vegetation phenology and temperature and precipitation showed obvious spatial differences. The EOS and LOS was mainly positively correlated with temperature. The results help to understand the spatiotemporal dynamic variations of vegetation photosynthetic phenology and the internal influencing mechanisms, and provide theoretical support for the construction and management of the ecological environment in the TNSFP region.
Keywords: *solar-induced chlorophyll fluorescence, vegetation photosynthetic phenology, spatiotemporal characteristics, driving force analysis; geographical detector*

Introduction

Vegetation, as a crucial component of terrestrial ecosystems, plays a pivotal role in climate change and also significantly influences the carbon and water cycles within them. Consequently, the dynamic shifts in vegetation have garnered widespread attention (Piao et al., 2019). Vegetation photosynthetic phenology refers to the adjustment of photosynthetic physiological rhythms by plants via photosynthesis for adapting to seasonal climate change, mainly encompassing the SOS, EOS of the vegetation growing season and the duration of the growing season (Yang et al., 2020). Essentially, it reflects

http://www.aloki.hu ● ISSN 1589 1623 (Print) ● ISSN 1785 0037 (Online)
DOI: http://dx.doi.org/10.15666/aeer/2303_47954826

the dynamic shifts within the ecosystem and the response of vegetation growth and development to environmental changes and it also serves as a vital indicator of both interannual variation in vegetation productivity and climate change (Zhou et al., 2016; Zhang et al., 2020). Moreover, alterations in vegetation photosynthetic phenology can impact climate-vegetation energy exchange (Lin et al., 2023), estimates of vegetation productivity (Xia et al., 2020), and the carbon balance of terrestrial ecosystems (Xu et al., 2022). Therefore, amidst persistent climate change, exploring the spatiotemporal characteristics and driving factors of vegetation photosynthetic phenology holds immense significance in terms of gauging the processes of carbon cycle, water cycle, and energy exchange between vegetation and the atmosphere.

Solar-induced chlorophyll fluorescence (SIF) is a fluorescence phenomenon emitted by chlorophyll molecules in photosynthetically active plants, and it has a positive correlation with photosynthesis (Zhao et al., 2023). As a bridge between photosynthesis and fluorescence signals, SIF provides a direct and more sensitive monitoring tool, which can reveal the physiological changes of vegetation and help to understand the impact of phenological changes on the ecosystem (Zhang et al., 2016). Meanwhile, SIF has unique advantages in monitoring the physiological characteristics of vegetation photosynthesis. It can not only detect the "actual photosynthesis" of vegetation, but also directly reflect the dynamic changes of actual photosynthesis in plants. It is less sensitive to factors such as clouds and atmosphere. It can understand the photosynthesis, growth, diseases, and stress status of plants through the fluorescence characteristics of plant photosynthesis (Zarco-Tejada et al., 2009). The research has found that SIF has great potential in the study of photosynthetic phenology of vegetation and can be used as a reliable data source, but its correlation with photosynthesis will vary according to different vegetation types (Anniwaer et al., 2014; Zhou et al., 2021). The difference ability of SIF in estimating phenology of different types of vegetation is actually the result of the joint influence of plant physiological mechanism, canopy structure, environmental factors and many other factors (Caparros-Santiago et al., 2021). Therefore, SIF has high application value in the estimation of vegetation photosynthetic phenology. The difference in its estimation ability reflects the unique physiological and ecological characteristics of vegetation types and their complex interaction with environmental factors (Yu et al., 2010; Cleland et al., 2012; Zhao et al., 2023).

Remote sensing technology plays a pivotal role in the study of vegetation photosynthetic phenology. It effectively monitors phenological changes across vast areas, thereby compensating for the limitations of traditional field observations in terms of coverage and methods. This technology provides crucial data support for exploring the spatiotemporal dynamics of vegetation photosynthetic phenology (Pettorelli et al., 2005). However, the majority of current vegetation phenology research relies on traditional vegetation indices, such as the Normalized Difference Vegetation Index (NDVI) and the Enhanced Vegetation Index (EVI), to examine the variations and influencing factors of vegetation phenology in diverse regions. Additionally, research methodologies exhibit a high degree of diversity (Cao et al., 2016). For example, Cong et al. (2022) conducted a study on the vegetation photosynthetic phenology in the Northern Hemisphere based on the GIMMS NDVI3g dataset and using the Pearson correlation analysis method. They found that the SOS and EOS of temperate vegetation in China are related to climate warming, and temperature plays a key role in both the SOS and EOS. Similarly, Fu et al. (2016) analyzed the vegetation phenological changes in the Greater Khingan Mountains and its various ecological sub-regions based on the GIMMS NDVI 3g dataset and found

http://www.aloki.hu ● ISSN 1589 1623 (Print) ● ISSN 1785 0037 (Online)
DOI: http://dx.doi.org/10.15666/aeer/2303_47954826

that they are more sensitive to temperature. These studies employ vegetation indices (VIs) to monitor the effects of climate change on vegetation photosynthetic phenology. However, these indices reflect the "potential photosynthesis" of vegetation and are significantly influenced by natural factors, including soil, clouds, and snow, which can potentially lead to deviations in detection accuracy (Liu et al., 2018; Li et al., 2019).

With the rapid development of observation satellites, such as greenhouse gases observing satellite (GOSAT), global ozone monitoring experiment 2 (GOME-2) and orbiting carbon observatory 2 (OCO-2), the inversion of vegetation photosynthetic phenology based on solar induced chlorophyll fluorescence (SIF) technology provides a new perspective for monitoring regional vegetation dynamic changes (Joiner et al., 2013, 2014; Guanter et al., 2014, 2015; Yoshida et al., 2015; Sun et al., 2017). Estimating vegetation photosynthetic phenology based on SIF data has become increasingly widespread. Jeong et al. (2017) estimated high-latitude forests based on SIF, NDVI, and gross primary productivity (GPP) data, and found that SIF was able to provide a more direct measurement of seasonal photosynthesis and a more accurate reflection of vegetation phenology. Joiner et al. analyzed different biotic communities in mid-latitude regions using GOSAT SIF, MODIS SIF, and NDVI data. Their study demonstrated that SIF data outperformed other datasets in capturing seasonal variations of actual photosynthesis across diverse vegetation types (Joiner et al., 2014). Zhou et al. (2024) estimated the vegetation photosynthetic phenology in Northeast China based on SIF, and found that SIF data could better reflect the true state of vegetation. Therefore, SIF is essential for revealing vegetation physiological changes and understanding the impact of phenological changes on the terrestrial ecosystems (Zhang et al., 2016).

The Three-North Shelter Forest Program (TNSFP) region is an important ecological security safeguard in northern China, and its ecological environment is relatively fragile, mainly covering most areas of Northeast, North, and Northwest China. With the continuous enhancement and implementation of the TNSFP, the ecological state of vegetation in this region has changed significantly, and the temporal-spatial dynamics of vegetation have received extensive attention. In recent years, many scholars' research on the Three-North region mainly focuses on the changes of vegetation coverage (Wang et al., 2012; Huang et al., 2016), primary productivity (An et al., 2020), and ecological quality of vegetation (Cao et al., 2017; Dao, 2019), while the research on photosynthetic phenology of vegetation in the Three-North Shelter Forest Program region is relatively scarce. In the context of global climate change, it is of great significance to closely monitor vegetation photosynthetic phenology for studying the growth and development of vegetation and evaluating the response of the ecosystem to climate change (Churkina et al., 2005; Kross et al., 2014). Therefore, by studying the dynamic change characteristics of vegetation photosynthetic phenology in the Three-North Shelter Forest Program region, the response laws between the dynamic changes of vegetation growth and meteorological and non-meteorological factors are explored.

Based on the solar-induced chlorophyll fluorescence data, meteorological data, topographic data, vegetation type data, and socio-economic data of the TNSFP region from 2001 to 2023, the dynamic thresholding technique was used to extract the phenological features of vegetation photosynthesis in the study area. Meantime, the methods of linear slope trend analysis, Coefficient of Variation (CV), and Hurst exponent were used to explore the spatiotemporal variation characteristics, vegetation ecological stability, and future trend projection of the vegetation photosynthetic phenology in the TNSFP region. The spatial heterogeneity and temporal variation driving forces of

http://www.aloki.hu ● ISSN 1589 1623 (Print) ● ISSN 1785 0037 (Online)
DOI: http://dx.doi.org/10.15666/aeer/2303_47954826

photosynthetic phenology in the TNSFP region were analyzed by using the geographical detector with optimal parameters and Pearson correlation analysis. The relevant research results can provide a theoretical basis for the vegetation phenology change characteristics and driving factors in the TNSFP region, effectively evaluate the carbon sequestration function of the vegetation in this area and its role in the global carbon cycle, and provide strong theoretical support for the vegetation rehabilitation and ecological environment construction of China's the northern terrestrial ecosystem.

Materials and methods

Study area

The TNSFP region (73°26'-137°50' E, 33°30'-50°12' N) is located in China's ecologically fragile zone. It spans 13 provinces (including autonomous regions and municipalities), namely Shaanxi, Gansu, Ningxia, Qinghai, Xinjiang, Shanxi, Hebei, Beijing, Tianjin, Inner Mongolia, Liaoning, Jilin, and Heilongjiang and 551 counties, covering approximately 407 million hectares, which account for 42.4% of China's total land area (Sa et al., 2023) (*Fig. 1*). Based on geomorphological features, the region is divided into four major construction zones: Northeast Region, North China Region, Loess Plateau Region, Inner Mongolia-Xinjiang Region, as defined by the China Forestry Regionalization (Zheng et al., 2013; Zhang and Zhang, 2024). The terrain of the TNSFP region slopes from high elevations in the west to lower elevations in the east and the altitude is between 100-5000 m. The region spans multiple climatic zones, with most areas experiencing a warm temperate continental monsoon climate. However, climatic variability is significant, including arid, semi-arid, and semi-humid climates. Arid and semi-arid areas constitute approximately two-thirds of the TNSFP region (Zhang and Chen, 2021). Annual average temperatures range from - 6°C to 15°C, and precipitation exhibits significant spatial variation, ranging from as little as 20 mm in the western areas to as much as 1100 mm in the eastern regions (Xie et al., 2020). This uneven distribution of precipitation results in deserts and rocky areas dominating the western parts, while forests and grasslands prevail in the eastern areas. The TNSFP region features diverse vegetation types, mainly including cultivated vegetation, grasslands, meadows, shrub, broad-leaved forests, and coniferous forests. In addition, thick growth of grass, mixed coniferous and broad-leaved forest, and alpine vegetation are sporadically distributed. (Wang et al., 2021) (*Fig. 1*).

Data sources and preprocessing

SIF data

This study utilized the GOSIF (Global OCO-2 SIF) dataset, a long-term remote sensing dataset spanning from 2001 to 2023 (Li and Xiao, 2019), available at http://globalecology.unh.edu. The GOSIF dataset offers a spatial resolution of 0.05°×0.05° and a temporal resolution of 8 days. It is generated using a data-driven model that integrates discrete SIF observations from OCO-2, MODIS remote sensing data, and reanalyzed meteorological data (Xiao et al., 2008; Gao et al., 2012). With strong spatial continuity, appropriate seasonal periodicity, and the ability to capture seasonal vegetation dynamics, GOSIF is highly effective for monitoring vegetation photosynthetic phenology (Guanter et al., 2012).

http://www.aloki.hu ● ISSN 1589 1623 (Print) ● ISSN 1785 0037 (Online)
DOI: http://dx.doi.org/10.15666/aeer/2303_47954826

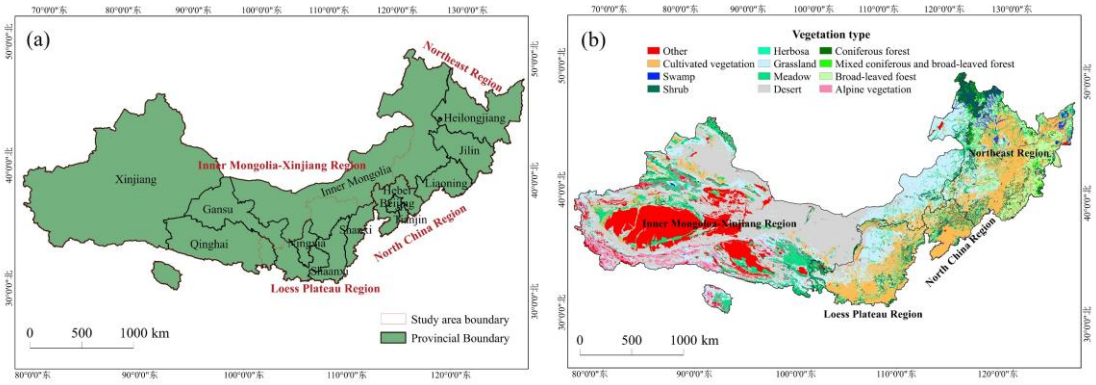

Figure 1. *Location and vegetation types of the study area*

Natural and socioeconomic data

The natural and socioeconomic data used in this study include terrain factors, meteorological factors, vegetation factors, and socioeconomic indicators. The detailed source of the data is shown in *Table 1*. The spatial resolution of elevation data is 90 m, and the slope and aspect data are extracted. The spatial resolution of vegetation type data and socio-economic data is 1 km. Meteorological data were obtained from the CRU website (*Table 1*). This dataset comprises monthly gridded data which are constructed on the basis of the monthly observational data calculated from daily data. These datasets have a spatial resolution of 0.05°×0.05° and a monthly temporal resolution. Meteorological data from 2001 to 2023 were processed into annual raster data using ArcGIS 10.8. The processing steps included cropping, projection transformation, pixel statistics, raster-to-point conversion, and inverse distance weighting (IDW) interpolation. To ensure consistency across all remote sensing datasets, the geographic coordinate system was uniformly set to the WGS 1984 coordinate system, and the data were resampled to a resolution of 1 km.

Table 1. *Data information*

Data type	Data name	Data sources
Terrain factors	Elevation Slope Aspect	AI Earth (https://engine-aiearth.aliyun.com/)
Meteorological factors	Annual average precipitation Annual average temperature Annual average maximum temperature Annual average minimum temperature	CRU (https://crudata.uea.ac.uk/cru/data/)
Vegetation factor	Vegetation type	Resource and Environmental Science Data Platform (https://www.resdc.cn)
Socioeconomic factor	Gross domestic product Population density	Resource and Environmental Science Data Platform (https://www.resdc.cn)

http://www.aloki.hu ● ISSN 1589 1623 (Print) ● ISSN 1785 0037 (Online)
DOI: http://dx.doi.org/10.15666/aeer/2303_47954826

Methods

Long-term vegetation phenology extraction

In this study, TIMESAT 3.3 software was used to fit long-term time-series curves for the TNSFP region from 2001 to 2023. The Savitzky-Golay (S-G) filtering method was employed to smooth GOSIF time-series curves, effectively removing noise and outliers to improve the accuracy of vegetation phenology retrieval. Meanwhile, with the help of TIMESAT 3.3 software, the dynamic threshold method was used to extract vegetation photosynthetic phenological parameters. The time when the SIF value reached a certain percentage of the SIF amplitude in the rising or falling stage was defined as the start period and the end period. It can set different thresholds for each pixel according to different dynamic conditions. Based on the threshold settings in previous studies, the threshold was set to 0.2. (Fensholt et al., 2012; Karkauskaite et al., 2017; Qiu et al., 2020). The selected vegetation photosynthetic phenological parameters are: the start of the growing season (SOS), the end of the growing season (EOS), and the length of the growing season (LOS).

$$SIF_t = \frac{SIF_t - SIF_{min}}{SIF_{max} - SIF_{min}} \times 0.2 \quad \text{(Eq.1)}$$

where: SIF_t represents the SIF value at time t; SIF_{max} and SIF_{min} represent the maximum and minimum values of SIF, respectively. LOS=EOS-SOS.

Analysis of linear trends in vegetation photosynthetic phenology

A univariate linear regression method was applied to analyze both the spatiotemporal trends in vegetation phenology across the study area from 2001 to 2023 and the interannual variation trends for different vegetation types (Yuan et al., 2021). The formula used is as follows:

$$Slope = \frac{n\sum_{i=1}^{n}(i \times Phe_i) - \sum_{i=1}^{n} i \times \sum_{i=1}^{n} Phe_i}{n\sum_{i=1}^{n} i^2 - (\sum_{i=1}^{n} i)^2} \quad \text{(Eq.2)}$$

where: Slope represents the regression slope of vegetation phenology (d/a); i represents the year; Phe_i represents the value of vegetation phenology in the i-th year (i =2001-2023); n represents the total number of years (n=23). If Slope<0, the SOS will advance or the LOS will shorten; if Slope>0, the SOS will be delayed or the LOS will be prolonged. The trend is examined using the F statistical method (Cao, 1988), where P represents the significance level with P<0.05 signifying a significant correlation and P>0.05 signifying an insignificant correlation.

Analysis of vegetation photosynthetic phenology stability and persistence

The coefficient of variation (CV) was used to evaluate the stability of vegetation phenology changes (Yao, 2022). It was applied to analyze fluctuations in vegetation photosynthetic phenology across the study area from 2001 to 2023. The formula used is as follows:

http://www.aloki.hu ● ISSN 1589 1623 (Print) ● ISSN 1785 0037 (Online)
DOI: http://dx.doi.org/10.15666/aeer/2303_47954826

$$CV = \frac{\sigma}{\mu} \quad \text{(Eq.3)}$$

where: CV represents the coefficient of variation; σ represents standard deviation of vegetation photosynthetic phenology parameters from 2001 to 2023; μ represents mean value of vegetation phenology parameters from 2001 to 2023. A smaller CV indicates lower fluctuation and higher stability in vegetation photosynthetic phenology.

In this study, the stability was classified into five levels to evaluate the spatial heterogeneity of phenological parameters: low fluctuation (CV<0.05), relatively low fluctuation (0.05≤CV<0.10), medium fluctuation (0.10≤CV<0.15), relatively high fluctuation (0.15≤CV<0.20）and high fluctuation (CV≥0.20).

The Hurst exponent was used to describe the future trends of long-term phenological parameter time series (Zhao et al., 2014). The R/S (rescaled range analysis) method was utilized to estimate the Hurst index, which could reflect the persistence of the vegetation phenological change trends at the pixel level across the study area.

The Hurst exponent (*H*) ranges between 0 and 1, *H* value can be divided into 3 intervals: if 0<*H*<0.5, it represents that the future trend of vegetation photosynthetic phenology will be opposite to the past, the time series manifests reverse persistence; If *H*=0.5, it represents that the future trend is unpredictable; If 0.5<*H*<1, it represents that the future trend of vegetation photosynthetic phenology will align with the past, and the time series presents positive persistence. A value closer to 1 indicates stronger persistence (Sen, 1968).

The results of Slope trend analysis and Hurst exponent analysis were overlaid to predict the persistence characteristics of future vegetation phenological trends in the study area. Future trend categories are detailed in *Table 2*.

Table 2. *Categories of future trends in change*

Slope	*H*-value	Future trend
Slope>0	0<*H*<0.5	From delay (extend) to advance (shorten)
	0.5<*H*<1	Continuous delay (extend)
Slope<0	0<*H*<0.5	From advance (shorten) to delay (extend)
	0.5<*H*<1	Continuous advance (shorten)

Driver analysis on spatial heterogeneity of vegetation photosynthetic phenology

The geographical detector method was applied to analyze the relationships between vegetation photosynthetic phenology and natural or socioeconomic factors, monitoring the spatial heterogeneity of vegetation photosynthetic phenology and identifying its main driving forces (Wang and Xu, 2017). Traditional geographical detectors require manual classification of continuous variables, which can be subject to subjective factors. Consequently, this study employed various discretization methods, including equal interval, natural breaks, quantile classification, geometric interval, and standard deviation, to classify continuous variables into 3-10 categories. The parameter combination yielding the highest *q*-value was selected to accurately identify key driving factors of vegetation photosynthetic phenology.

http://www.aloki.hu ● ISSN 1589 1623 (Print) ● ISSN 1785 0037 (Online)
DOI: http://dx.doi.org/10.15666/aeer/2303_47954826

This study used factor detection, interaction detection, risk detection, and ecological detection within the optimal parameter geographical detector to analyze, from a spatial perspective, the impacts of driving factors on vegetation photosynthetic phenology (SOS, EOS, LOS) and to explore the interactions among each factor. Driving factors included elevation, slope, aspect, annual average precipitation, annual average temperature, annual maximum temperature, annual minimum temperature, vegetation type, gross domestic product, and population density. These factors were used as independent variables (*X*), while vegetation photosynthetic phenology metrics (SOS, EOS, LOS) were used as dependent variables (*Y*).

Single-factor detection

Single-factor detection evaluates the explanatory power of driving factors (*X*) on vegetation photosynthetic phenology metrics (*Y*).

$$q = 1 - \frac{\sum_{h=1}^{L} N_h \sigma_h^2}{N\sigma^2} = 1 - \frac{SSW}{SST} \quad \text{(Eq.4)}$$

$$SSW = \sum_{h=1}^{n} N_h \sigma_h^2, SST = N\sigma^2 \quad \text{(Eq.5)}$$

where: q represents the explanatory power of driving factors. The value range of q is [0, 1]; A q-value closer to 1 indicates that the driving factors (*X*) have a stronger explanatory power for vegetation photosynthetic phenology (*Y*), and a lower value indicates weaker explanatory power. h represents category index (h=1,2,3, …); L represents the stratification of the variable *Y* or factor *X*; N_h and N respectively represent the number of units in layer h and the total number of units in the entire area; $\sigma^2$and σ_h^2 respectively represent the variances of *Y* values in the entire area and layer *h*; *SSW* and *SST* respectively represent the sum of the variances within layer *h* and the total variance in the entire area.

Interaction detection

Interaction detection is chiefly employed to painstakingly scrutinize the interactive impacts among assorted driving factors, juxtapose the explanatory potency of two driving factors operating in concert on vegetation photosynthesis phenology *Y* with that of a single driving factor, and ascertain whether the synergistic influence of two distinct factors *X*1 and *X*2 on vegetation photosynthesis phenology *Y* is intensified or attenuated. The specific types of interaction among the detection factors are presented in *Table 3*.

Ecological detection

Ecological detection examines whether there is a significant spatial difference in the impact of two driving factors (*X*1 and *X*2) on the spatial distribution of vegetation photosynthetic phenology (*Y*). The significance of these spatial differences is measured using the F-statistic.

http://www.aloki.hu ● ISSN 1589 1623 (Print) ● ISSN 1785 0037 (Online)
DOI: http://dx.doi.org/10.15666/aeer/2303_47954826

Table 3. *Specific interactions of detection factors*

Distinguish basis	Interaction
$q(X1\cap X2)<\text{Min}[q(X1), q(X2)]$	Nonlinear weakening
$\text{Min}[q(X1), q(X2)]<q(X1\cap X2)<\text{Max}[q(X1), q(X2)]$	Single factor nonlinear weakening
$q(X1\cap X2)<\text{Max}[q(X1), q(X2)]$	Two-factor enhancement
$q(X1\cap X2)=q(X1)+q(X2)$	Independence
$q(X1\cap X2)<q(X1)+q(X2)$	Non-linear enhancement

Min[$q(X1)$, $q(X2)$]: Take the minimum value between q ($X1$) and q ($X2$); Max[$q(X1)$, $q(X2)$]: Take the maximum value between q ($X1$) and q ($X2$); $q(X1)+q(X2)$: Sum q ($X1$) and q ($X2$); $q(X1\cap X2)$: q ($X1$), q ($X2$) interact with each other

Risk detection

Risk detection primarily aims to identify the distribution scope of the driving factors that give rise to alterations in vegetation photosynthesis phenology and employs the T statistic to evaluate whether there are substantial disparities in the attribute means among sub-regions.

Driver analysis on temporal variations of vegetation photosynthetic phenology

The correlation between meteorological elements (precipitation, average temperature, average maximum temperature, average minimum temperature) and vegetation photosynthetic phenology was analyzed based on Pearson correlation coefficient method. The correlation coefficient r is used to express the correlation of vegetation photosynthetic phenology and meteorological elements. The calculation formula is as follows:

$$r=\frac{\sum_{i=1}^{n}(x_i-\bar{x})(y_i-\bar{y})}{\sqrt{\sum_{i=1}^{n}(x_i-\bar{x})^2}\sqrt{\sum_{i=1}^{n}(y_i-\bar{y})^2}} \quad \text{(Eq.6)}$$

where: r is the correlation coefficient between variable x and variable y, x_i and y_i are the values of variable x and variable y in the i year, respectively, $\bar{x}$ and $\bar{y}$ are the multi-year mean values of variable x and variable y, respectively, and N is the number of research years (n=23). The value range of Pearson correlation coefficient r ranges from -1 to 1. If r>0, it means that variable x is positively correlated with variable y, if r<0, it means that variable x is negatively correlated with variable y. The closer r is to 1, the stronger the correlation between the two variables. According to the results of the t-test, if the correlation passes the 0.05 confidence level, it is considered a significant correlation.

Data statistics and analysis

ArcGIS 10.8 software is used to preprocess spatial data such as SIF data, meteorological data, as well as natural and social data. Excel software is used to complete data sorting and outlier removal. MATLAB R2018b software is used to smooth the long-time series data based on the TIMESAT 3.3 platform, and the dynamic threshold method is used to accurately extract the start and end periods of vegetation phenology. The

http://www.aloki.hu ● ISSN 1589 1623 (Print) ● ISSN 1785 0037 (Online)
DOI: http://dx.doi.org/10.15666/aeer/2303_47954826

geographic detector package (gtdb_v1.2) in R 4.1.2 is used to analyze the spatial heterogeneity of vegetation photosynthetic phenology. At the same time, this software is used to analyze the temporal change of vegetation photosynthetic phenology, which reveals the impact of various driving factors on vegetation phenology in the study area. Finally, ArcGIS software and Origin 2024 software are used to draw spatial distribution maps, frequency distribution maps, and inter-annual change trend maps, etc.

Results and analysis

Spatial distribution pattern of vegetation photosynthetic phenology

The multi-year average spatial distribution patterns of spring photosynthetic phenology (SOS), autumn photosynthetic phenology (EOS), and growing season length (LOS) in the TNSFP region from 2001 to 2023 are shown in *Fig. 2*.

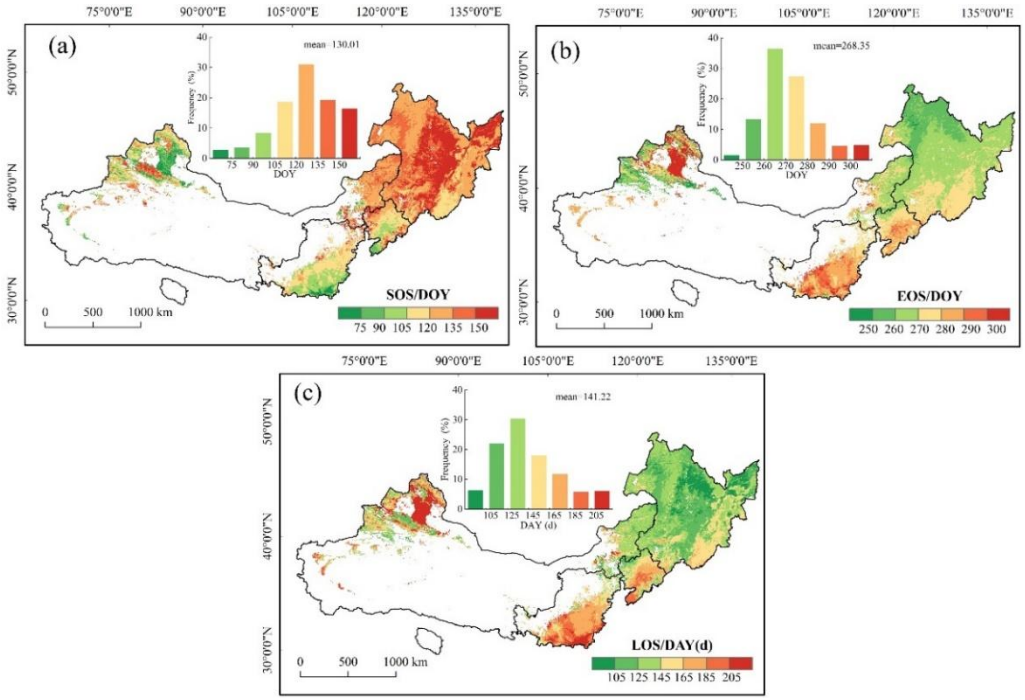

Figure 2. *Spatial and frequency distribution patterns of vegetation photosynthetic phenology in the TNSFP region from 2001 to 2023*

The SOS values were predominantly concentrated within the range of 105 to 150 DOY (day of the year), corresponding to mid-April to late May, with an average SOS value of 130.01 DOY. These values were mainly distributed in the southwestern and southeastern parts of the Northeast Region and the eastern part of the Inner Mongolia-Xinjiang Region. Regions with earlier SOS (<105 DOY) were located in the northwestern Inner Mongolia-Xinjiang Region and the southern Loess Plateau Region. Areas with later SOS (>150 DOY) were found in the central Northeast Region, accounting for 16.41% of the total study area. The EOS values were primarily concentrated within the range of 250 to 290 DOY, corresponding to early September to mid-October, with an average EOS value of 268.35 DOY. EOS was mainly observed in the Northeast Region, the southern North

http://www.aloki.hu ● ISSN 1589 1623 (Print) ● ISSN 1785 0037 (Online)
DOI: http://dx.doi.org/10.15666/aeer/2303_47954826

China Region, and the southeastern Loess Plateau Zone. The LOS values concentrated in the range of 105 to 185 days, that is, from mid-April to early July, with a mean LOS of 141.22 days. Regions with longer growing seasons (>185 days) were located in small parts of the northwestern Inner Mongolia-Xinjiang Region and the southern Loess Plateau Region. Shorter LOS (<105 days) was primarily concentrated in the central Northeast Region. From an overall perspective, the Northeast Region showed later SOS, earlier EOS, and shorter LOS compared to other regions.

Statistical analysis of multi-year mean phenological parameters from 2001 to 2023 for different vegetation types in the TNSFP region is shown in *Table 4*. There are significant differences in the SOS, EOS, and LOS among different vegetation types. The SOS of alpine vegetation and herbosa was the earliest, 105.38 DOY and 113.24 DOY, respectively, followed by shrub, coniferous forest, coniferous and broad-leaved mixed forest, broad-leaved forest and grassland. The SOS of meadow and cultivated vegetation was the latest, 132.40 DOY and 132.13 DOY, respectively. The end time of EOS in coniferous forest was the earliest, 263.74 DOY, followed by coniferous and broad-leaved mixed forest, broad-leaved forest and meadow, and the end time was between 260 and 270 DOY. The EOS in grassland, alpine vegetation, shrub and cultivated vegetation was later, while the EOS in herbosa was the latest, 282.05 DOY. The LOS is jointly determined by the SOS and EOS. Meadows and coniferous forests have the shortest LOS, with mean durations of 134.31 days and 138.71 days respectively. Conversely, alpine vegetation and herbosa demonstrate the longest LOS, extending to 167.10 days and 168.51 days, respectively.

Table 4. *Statistics on multi-year mean values of vegetation photosynthetic phenology from different vegetation types in the TNSFP region from 2001 to 2023*

Vegetation Type	SOS(DOY)	EOS(DOY)	LOS(d)
Grassland	126.92	271.75	144.48
Meadow	132.40	267.10	134.31
Herbosa	113.24	282.05	168.51
Shrub	122.77	273.81	150.69
Cultivated vegetation	132.13	274.21	141.72
Alpine vegetation	105.38	272.60	167.10
Coniferous forest	124.58	263.74	138.71
Broad-leaved forest	125.92	268.22	141.85
Mixed coniferous and broad-leaved forest	124.83	266.19	140.87

Spatiotemporal evolution characteristics of vegetation photosynthetic phenology

The spatial trends of SOS, EOS, and LOS in the TNSFP region from 2001 to 2023 are shown in *Fig. 3*. From a spatial perspective, the SOS generally exhibited an advancing trend across the study area, but most regions showed no significant changes. Significant advancements in SOS were primarily observed in the southeastern part of the Northeast Region, with 20.84% showing significant advance of the total area (P<0.05). The EOS displayed an overall delaying trend, with delays concentrated in the southeastern and central parts of the Northeast Region. In contrast, an advancing trend was observed in the northern part of the Northeast Region, covering approximately 35.54% of the total study

http://www.aloki.hu ● ISSN 1589 1623 (Print) ● ISSN 1785 0037 (Online)
DOI: http://dx.doi.org/10.15666/aeer/2303_47954826

area, while a small portion of the southern Inner Mongolia-Xinjiang Region exhibited a significantly advanced trend (P<0.05), accounting for only 5.67% of the area. The overall LOS showed a general extension trend, with 26.76% of the area experiencing a significant extending of the growing season (P<0.05). However, the northern part of the Northeast Region exhibited a slight shortening trend. These trends reflect the complex regional differences in the spatial dynamic changes of vegetation photosynthetic phenology within the study area.

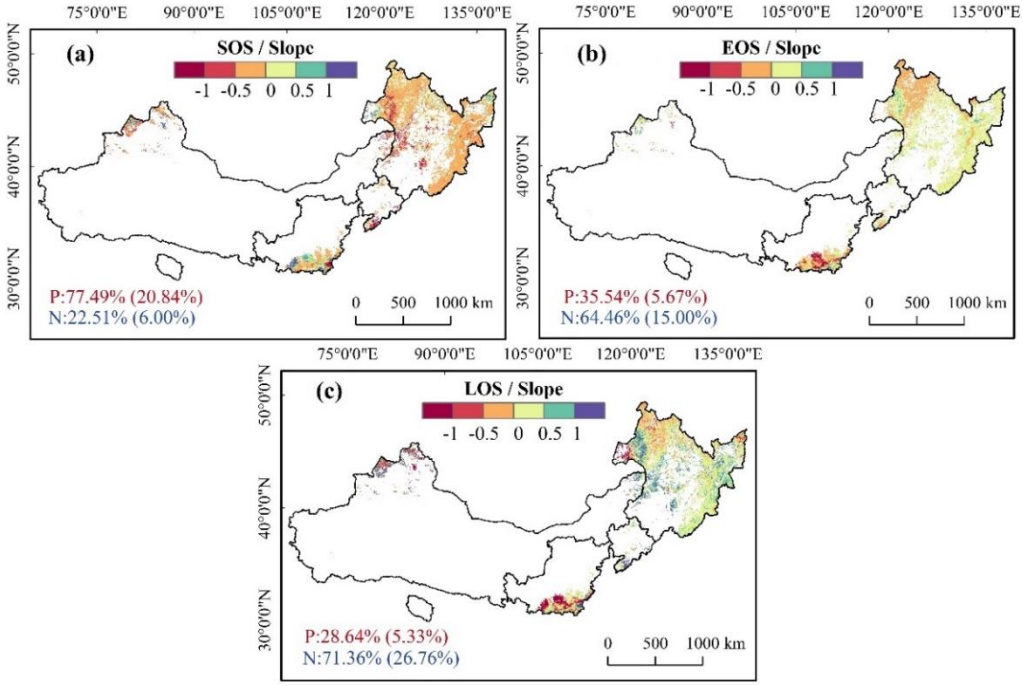

Figure 3. *Spatial variation trends of vegetation photosynthetic phenology in the TNSFP region from 2001 to 2023.The red text (P) represents a positive correlation indicating the SOS, EOS advanced or the LOS shortened. The blue text (N) represents a negative correlation indicating the SOS, EOS is delayed or the LOS extended. The values in parentheses represent the proportion of significantly correlated pixels (P<0.05)*

The overall interannual variation characteristics of vegetation photosynthetic phenology in the TNSFP region from 2001 to 2023 are shown in *Fig. 4*. From 2001 to 2023, the interannual variation of the SOS in TNSFP exhibited a significant advancing trend (P<0.05) at a rate of 0.16 d/a. The average value of SOS ranged from 127.05 to 134.98 DOY, with the earliest start recorded in 2020 (127.05 DOY) and the latest in 2011 (134.98 DOY). The interannual variation of EOS in TNSFP displayed a highly significant delaying trend (P<0.01) at a rate of 0.20 d/a. The earliest EOS occurred in 2002 (264.02 DOY), while the latest was observed in 2023 (272.31 DOY). The interannual variation of the LOS showed a significant extending trend (P<0.05) at a rate of 0.26 d/a. The shortest LOS was recorded in 2011, and the longest in 2009, with a difference of 14.51 days between the two years.

http://www.aloki.hu ● ISSN 1589 1623 (Print) ● ISSN 1785 0037 (Online)
DOI: http://dx.doi.org/10.15666/aeer/2303_47954826

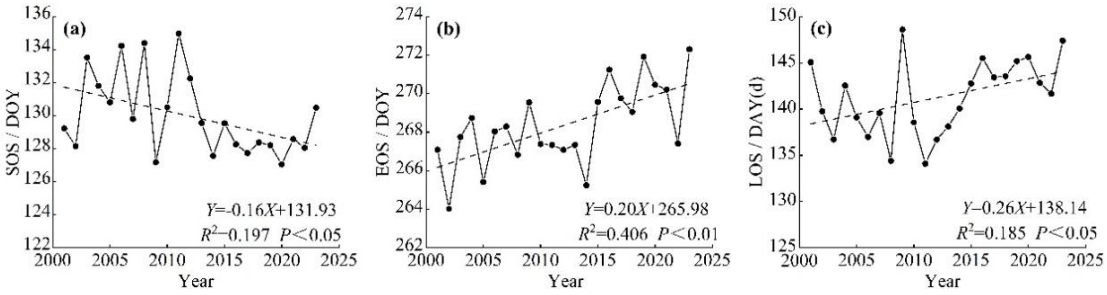

Figure 4. *Interannual variation trends of vegetation photosynthetic phenology in the TNSFP region from 2001 to 2023*

Temporal variation trends of phenological phases for different vegetation types

The interannual variation trends and fitted equations for phenological characteristics across different vegetation types in the TNSFP region are shown in *Fig. 5* and *Table 5*.

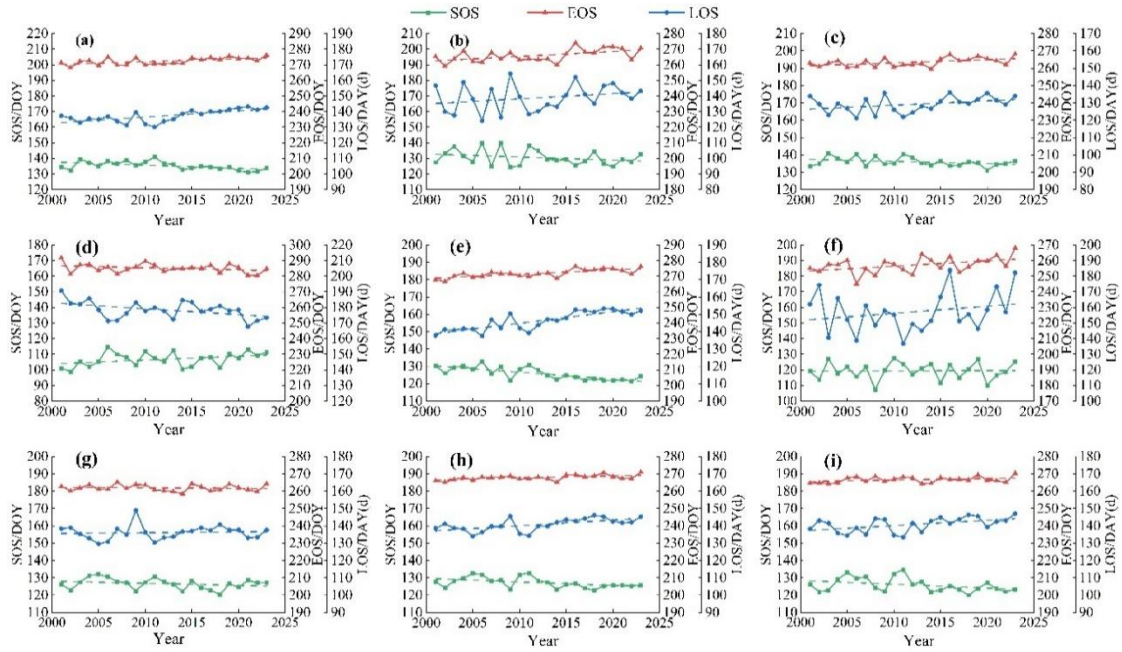

Figure 5. *Interannual variations of vegetation photosynthetic phenology for different vegetation types in the TNSFP region from 2001 to 2023. (a): cultivated vegetation; (b): grassland; (c): meadow; (d): herbosa; (e): shrub; (f): alpine vegetation; (g): coniferous forest; (h): broad-leaved forest; (i): mixed coniferous and broad-leaved forest*

The SOS of cultivated vegetation, grasslands, meadows, shrub, coniferous forests, and mixed coniferous and broad-leaved forests exhibited advancing trends. Among these, shrubs and cultivated vegetation showed a highly significant advancing trend, while broad-leaved forests displayed a significant advancing trend, with rates of 0.40 d/a, 0.21 d/a, and 0.21 d/a, respectively. In contrast, grass clumps, alpine vegetation, and broad-leaved forests exhibited slight delayed trends.

http://www.aloki.hu ● ISSN 1589 1623 (Print) ● ISSN 1785 0037 (Online)
DOI: http://dx.doi.org/10.15666/aeer/2303_47954826

Table 5. *Variation trend fitting of vegetation photosynthetic phenology for different vegetation types in the TNSFP region from 2001 to 2023*

Vegetation type	SOS		EOS		LOS	
	Fitting equation	R^2	Fitting equation	R^2	Fitting equation	R^2
Grassland	Y=-0.19X+132.81	0.072	Y=0.32X+262.17	0.286**	Y=0.33X+134.85	0.068
Meadow	Y=-0.13X+137.52	0.121	Y=0.18X+261.31	0.249*	Y=0.25X+236.12	0.140
Herbosa	Y=0.25X+103.76	0.140	Y=-0.14X+286.75	0.106	Y=-0.38X+182.97	0.225*
Shrub	Y=-0.40X+130.55	0.574**	Y=0.28X+268.43	0.554**	Y=0.67X+138.16	0.713**
Cultivated vegetation	Y=-0.21X+137.76	0.290**	Y=0.20X+270.01	0.352**	Y=0.40X+132.48	0.484**
Alpine vegetation	Y=0.02X+119.02	0.001	Y=0.34X+252.97	0.211*	Y=0.46X+151.61	0.058
Coniferous forest	Y=-0.12X+128.02	0.072	Y=-0.02X+262.09	0.007	Y=0.05X+135.50	0.007
Broad-leaved forest	Y=0.21X+129.71	0.226*	Y=0.12X+266.32	0.322**	Y=0.33X+136.76	0.389**
Mixed coniferous and broad-leaved forest	Y=-0.22X+128.46	0.134	Y=0.09X+265.46	0.125	Y=0.31X+137.00	0.253*

* represents significant (P<0.05), * * represents highly significant (P<0.01)

For EOS, all vegetation types except grass clumps and coniferous forests showed significant delayed trends. Cultivated vegetation, grasslands, shrub, and broad-leaved forests showed highly significant delayed trends, with alpine vegetation exhibiting the most pronounced delayed trend at a rate of 0.34 d/a.

The LOS of cultivated vegetation, shrublands, and broad-leaved forests showed highly significant extended trends, with rates of 0.40 d/a, 0.67 d/a, and 0.33 d/a, respectively. Grass clumps and mixed conifer-broadleaf forests displayed significant extended trends. However, grasslands, meadows, alpine vegetation, and coniferous forests exhibited slight shortened trends, with grass clumps showing a significant shortened trend at a rate of 0.38 d/a.

Stability and future trends of vegetation phenological phases

The coefficient of variation (CV) was calculated on a pixel-by-pixel basis to evaluate the fluctuation state in vegetation photosynthetic phenology over the past 23 years in the TNSFP region (*Fig. 6*). From 2001 to 2023, the SOS and EOS exhibited generally low fluctuation levels across the study area. The LOS in the study area was in a state of low and relatively low fluctuation, accounting for 90.62% and 6.20% of the total area of the study area, respectively. The relatively low fluctuation is sporadically distributed in the northwest and central parts of the Northeast Region, as well as in the southern part of the Loess Plateau Region. These findings suggest that the stability of vegetation photosynthetic phenology is high overall, with localized variability in specific regions.

The sustainability of future trends in SOS, EOS, and LOS of vegetation in the TNSFP region is analyzed through the Hurst index (*Fig. 7*). The range of H values for SOS in the study area ranges from 0.02 to 0.86, with a mean of 0.41. Areas with H values between 0 and 0.5 account for 81.83% of the total area, indicating that the future trend of the SOS in most regions is opposite to the past, exhibiting a delayed trend. The range of H values for EOS in the study area is between 0.07 and 0.82, with a mean of 0.38. Areas with H

http://www.aloki.hu ● ISSN 1589 1623 (Print) ● ISSN 1785 0037 (Online)
DOI: http://dx.doi.org/10.15666/aeer/2303_47954826

values between 0 and 0.5 account for 86.55% of the total area, suggesting that the future trend of the EOS in the study area is contrary to the past, exhibiting a shortening trend. Only a few regions have EOS with an *H* value greater than 0.5, indicating that the EOS in these areas will continue to exhibit a delayed change trend in the future. The *H* value of LOS in the study area ranges from 0.04 to 0.79, with a mean of 0.42. Areas with H values between 0 and 0.5 account for 80.77%, indicating that 80.77% of the LOS in the study area will change in the future in the opposite direction to the past, showing a shortening trend. Areas with *H* values between 0.5 and 1 account for 19.23%, suggesting that the change trend of LOS in the future will be similar to that of the past 23 years, continuing to extend.

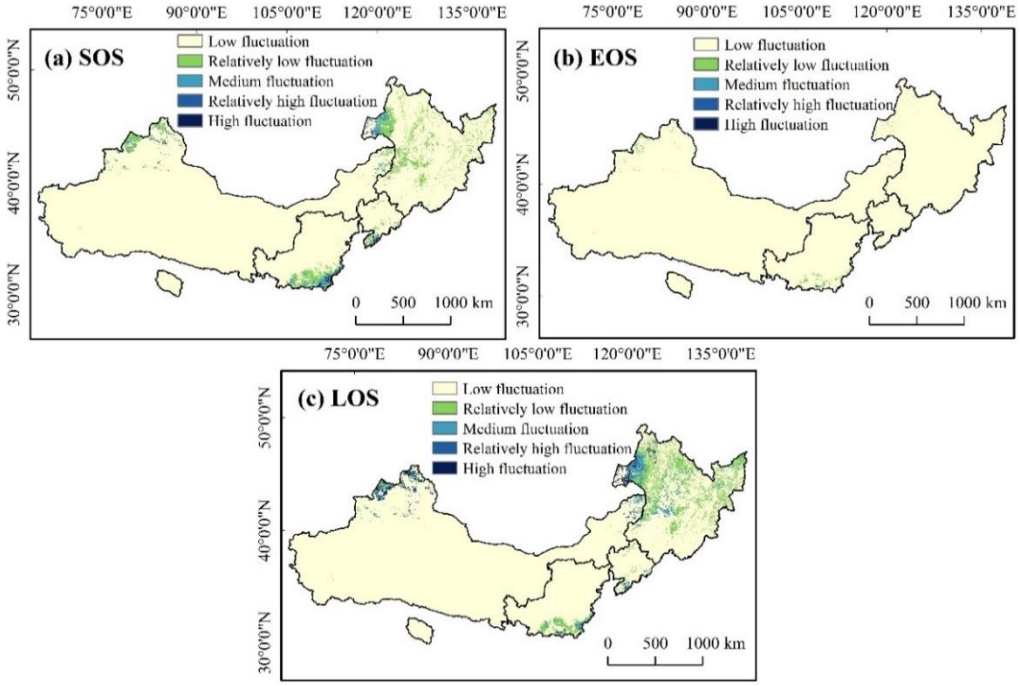

Figure 6. *Stability of vegetation photosynthetic phenology in the TNSFP region from 2001 to 2023*

By overlaying the Slope trend with the Hurst index, four future trends of vegetation photosynthetic phenology in the TNSFP region are obtained (*Fig. 8*). The area where the trend of the SOS of the vegetation changes from advancing to delaying in the future is the largest, accounting for approximately 63.62% of the total area. It is mainly concentrated in the Northeast Region, the southeastern part of the North China Region and the southernmost part of the Loess Plateau Region. This is followed by a continuous delaying trend, accounting for 18.21%, mainly distributed in the western part of the Northeast Region. The area where the EOS of vegetation exhibits a shift from a delayed to an advanced trend occupies the largest proportion, which is 41.29%, of the total area of the study area. It is chiefly concentrated in the southeastern and central areas of the Northeast Region. Meanwhile, an area accounting for 25.49% shows a trend changing from advanced to delayed, mainly distributed in the northern part of the Northeast Region and the southernmost section of the Loess Plateau Region. The proportion of areas where the LOS shows a trend from elongation to shortening is 61.99%, mainly distributed in the

http://www.aloki.hu ● ISSN 1589 1623 (Print) ● ISSN 1785 0037 (Online)
DOI: http://dx.doi.org/10.15666/aeer/2303_47954826

Northeast Region and scattered in the North China Region; The proportion of regions showing a trend from shortening to extending is 23.78%, mainly distributed in the western and northernmost parts of the Northeast Region. The areas showing a continuous extending trend and a continuous shortening trend are the least, accounting for 12.82% and 7.60% of the total area, respectively.

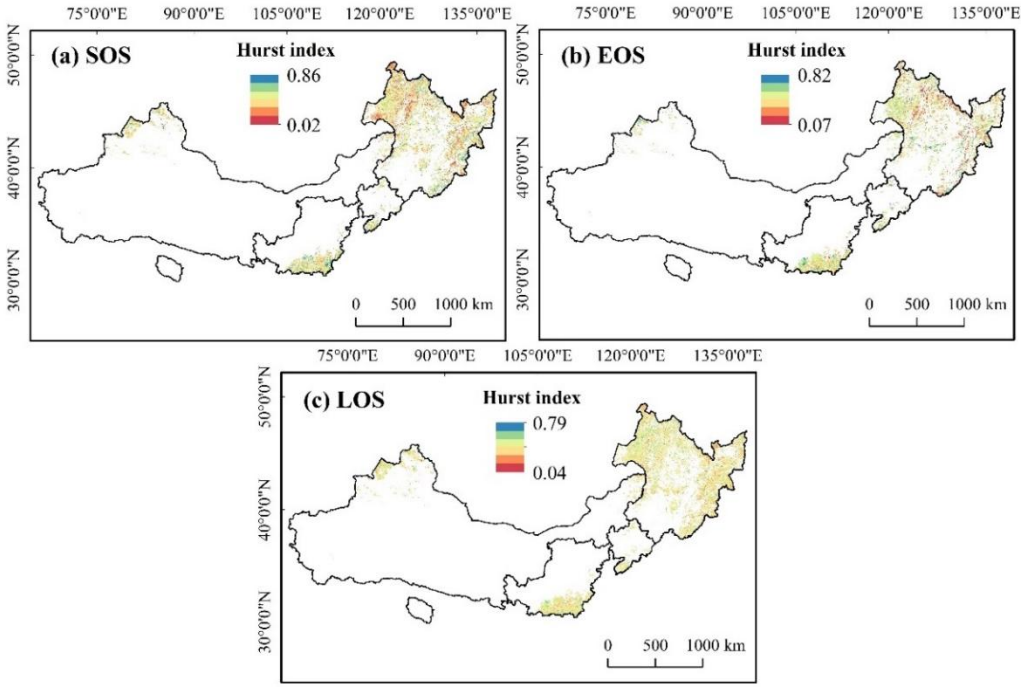

Figure 7. *Spatial distribution of Hurst index of vegetation photosynthetic phenology in the TNSFP region*

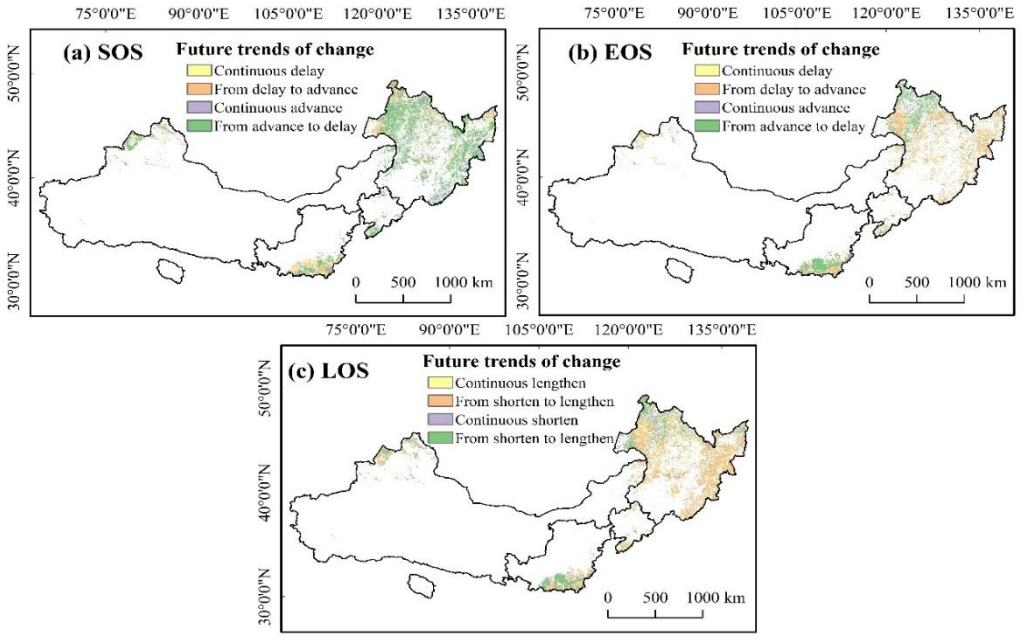

Figure 8. *Spatial distributions of future trends in vegetation photosynthetic phenology in the TNSFP region*

http://www.aloki.hu ● ISSN 1589 1623 (Print) ● ISSN 1785 0037 (Online)
DOI: http://dx.doi.org/10.15666/aeer/2303_47954826

Driver analysis on vegetation photosynthetic phenology

Driver analysis on spatial heterogeneity

Single-factor detection

The results of single-factor detection reveal the explanatory power (q-values) of individual driving factors for SOS, EOS, and LOS (*Fig. 9*).

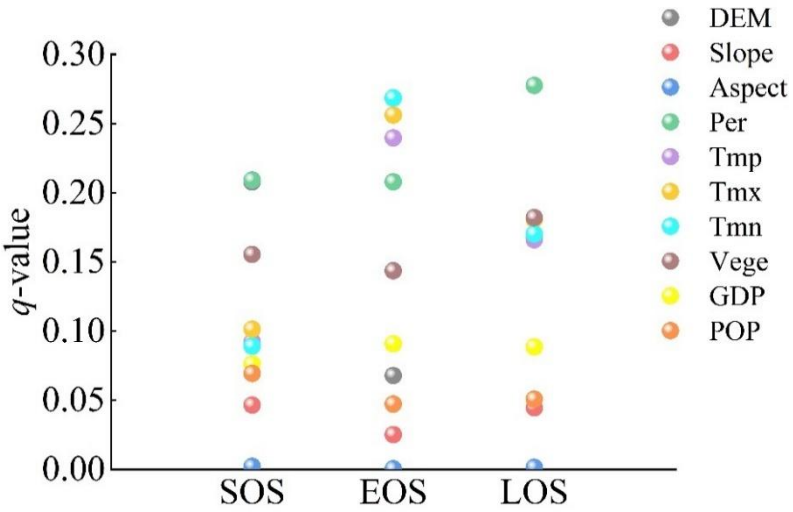

Figure 9. *Single-factor detection results of vegetation photosynthetic phenology in the TNSFP region (q). DEM: elevation; Per: annual precipitation; Tmp represents annual average temperature; Tmx: annual maximum temperature; Tmn: annual minimum temperature; Vege: vegetation type; GDP: gross domestic product; POP: population density*

For SOS, the driving factors were ranked by explanatory power as follows: precipitation, elevation, vegetation type, maximum temperature, average temperature, minimum temperature, gross domestic product, population density, slope, and aspect. Natural factors dominated, with precipitation showing the highest explanatory power (q=0.209), followed closely by elevation (q=0.208). Vegetation type and maximum temperature also had notable influences (q=0.155 and 0.101, respectively).

For EOS, the driving factors were ranked by explanatory power as follows: minimum temperature, maximum temperature, average temperature, precipitation, vegetation type, gross domestic product, elevation, population density, slope, and aspect. Among them, annual minimum temperature has the greatest impact on the EOS (q=0.269), followed by maximum temperature, average temperature, and precipitation (q>0.200).

For LOS, the driving factors were ranked by explanatory power as follows: annual precipitation, vegetation type, maximum temperature, minimum temperature, elevation, average temperature, gross domestic product, population density, slope, and aspect. Annual precipitation is the strongest factor in explaining LOS (q=0.278), followed by vegetation type, maximum temperature, minimum temperature, elevation, and average temperature, which have relatively high explanatory power for LOS (q>0.150). The explanatory power of slope, aspect, gross domestic product, and population density for the SOS, EOS, and LOS is relatively weak (q<0.100).

http://www.aloki.hu ● ISSN 1589 1623 (Print) ● ISSN 1785 0037 (Online)
DOI: http://dx.doi.org/10.15666/aeer/2303_47954826

Interaction detection

Using interaction detectors to explore the interactions among driving factors of the SOS, EOS, and LOS facilitates the evaluation of the influence extent of the synergistic effect of two factors on vegetation photosynthetic phenology (*Fig. 10*). The results indicate that the interaction between any two driving factors had a stronger impact on vegetation photosynthetic phenology than individual factors, showing nonlinear enhancement or bilinear enhancement. There is no mutually independent and weakening relationship, suggesting that vegetation photosynthetic phenology in the TNSFP region is influenced by the interplay of multiple factors. The interaction of Precipitation with other driving factors had a stronger explanatory power for SOS and LOS compared to single-factor effects. Similarly, the interaction of minimum temperature with other factors enhanced its influence on the EOS. This clearly confirms that precipitation is a key factor for SOS and LOS, while minimum temperature is critical for EOS, consistent with the results of single-factor detection. Slope, aspect, gross domestic product and population density have a weak impact on the vegetation photosynthetic phenology alone (low *q* value), but the q value has increased after interaction with other driving factors, indicating that the interaction between the relatively weak single factors and other driving factors can significantly enhance the explanatory power for vegetation photosynthetic phenology in the region.

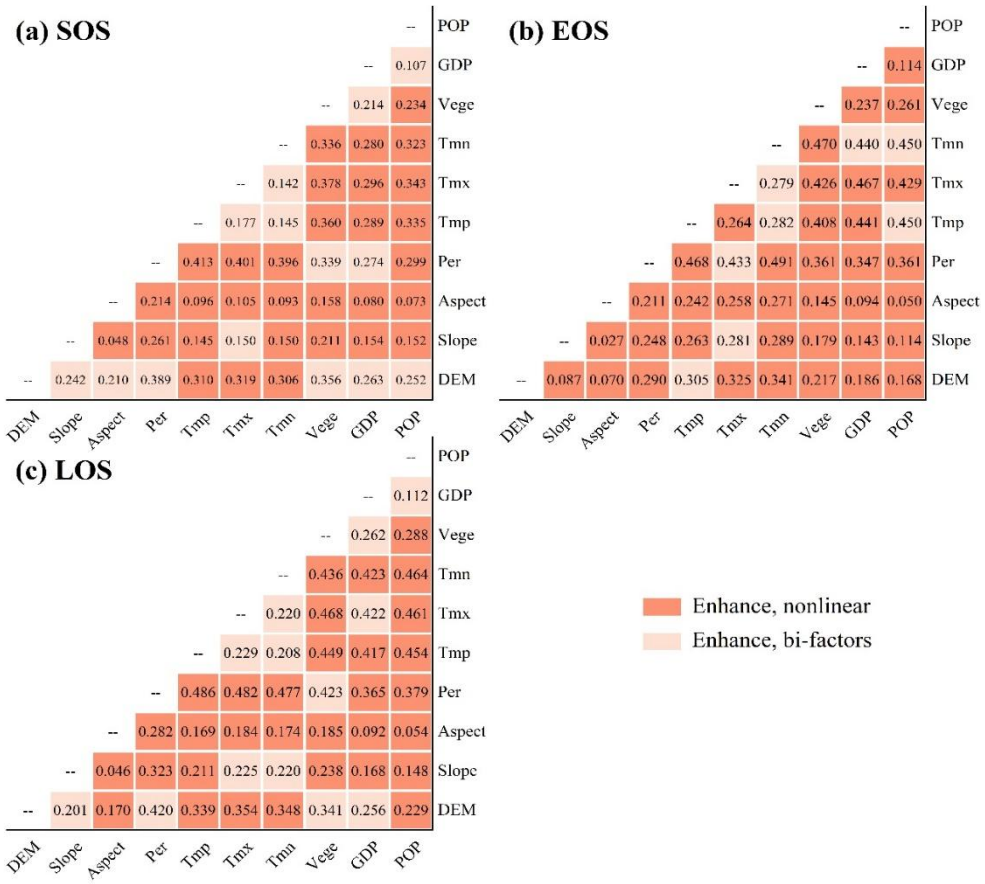

Figure 10. *Interaction detection results of vegetation photosynthetic phenology in the TNSFP region. DEM: elevation; Per: annual precipitation; Tmp represents annual average temperature; Tmx: annual maximum temperature; Tmn: annual minimum temperature; Vege: vegetation type; GDP: gross domestic product; POP: population density*

http://www.aloki.hu ● ISSN 1589 1623 (Print) ● ISSN 1785 0037 (Online)
DOI: http://dx.doi.org/10.15666/aeer/2303_47954826

For SOS, the interaction between precipitation and average temperature had the strongest impact (q=0.413), followed by the interaction between precipitation and maximum temperature (q=0.40). For EOS, the interaction between minimum temperature and precipitation was most influential (q=0.491), followed by minimum temperature and vegetation type (q=0.47). For LOS, the strongest interaction was between precipitation and average temperature (q=0.48), with precipitation and maximum temperature as the second strongest (q=0.48).

Ecological factor detection

Significance testing of was conducted using an ecological detector to investigate the impacts of two factors on the spatial distribution of vegetation photosynthetic phenology. The results showed that both factors had significant differences in their impacts on the spatial distribution of vegetation photosynthetic phenology.

Risk factor detection

This study selected the six drivers exerting the most significant influence on the photosynthetic climate of vegetation for risk detection: precipitation, minimum temperature, maximum temperature, average temperature, elevation, and vegetation type. The risk detection was utilized to explore the maximum range of distributions and the minimum range of distributions of alterations in the SOS, EOS, and LOS by the drivers (*Tables 6, 7, Figure 11*).

Table 6. *Maximum distribution range of vegetation photosynthetic phenology changes due to driving factors`*

Factors	SOS		EOS		LOS	
	Range	Mean (DOY)	Range	Mean (DOY)	Range	Mean (d)
Elevation	2420~6400m	104.93	-156~1.4m	297.37	-156~1.65m	189.65
Precipitation	140~219mm	100.53	141~219mm	296.19	140~219mm	200.25
Average temperature	11.10~14.50℃	113.19	12.10~14.50℃	286.01	10.60~12.50℃	173.92
Maximum temperature	16.80~18.60℃	110.13	15.90~17.50℃	286.24	15.10~20.40℃	175.05
Minimum temperature	6.67~8.84℃	108.53	2.66~4.68℃	287.21	3.82~8.84℃	175.53
Vegetation type	Herbosa	116.48	Herbosa	281.84	Herbosa	165.75

When the elevation is below 344 m, the SOS displays a delaying trend with increasing elevation, while when the elevation is higher than 344 m, the SOS manifests an advancing trend with increasing elevation. When the precipitation is between 140 and 435 mm, the SOS exhibits a delaying trend with increasing precipitation, and when the precipitation is greater than 435 mm, the SOS presents an advancing trend with increasing precipitation. When the average temperature is greater than 4.5°C, the SOS demonstrates an advancing trend with increasing average temperature and vice versa. When the maximum temperature is between 7.82 and 18.6℃, the SOS reveals an advancing trend with decreasing of maximum temperature. When the minimum temperature is higher than -

http://www.aloki.hu ● ISSN 1589 1623 (Print) ● ISSN 1785 0037 (Online)
DOI: http://dx.doi.org/10.15666/aeer/2303_47954826

6.36℃, the SOS shows an advancing trend with decreasing minimum temperature, and vice versa, it displays a delaying trend.

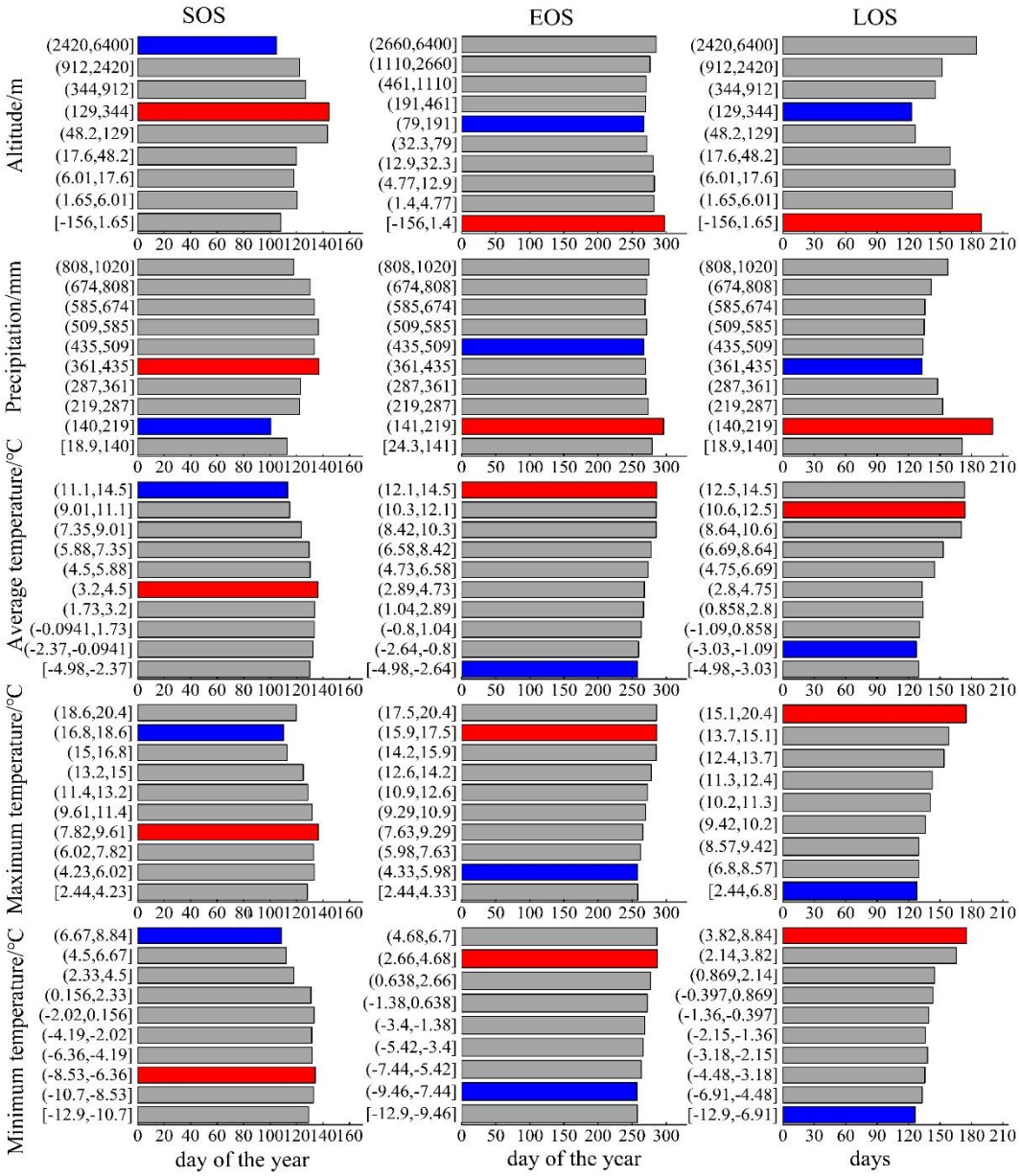

Figure 11. *Risk factor detection results of different vegetation photosynthetic phenology*

When the elevation is lower than 191 m, the EOS shows an advancing trend with increasing elevation, and when the elevation is higher than 191m, it manifests a delaying trend with increasing elevation. When precipitation is between 141 and 509 mm, the EOS presents an advancing trend with increasing precipitation, and when it is greater than 509 mm, the EOS displays a delaying trend with increasing precipitation. The average temperature, the maximum temperature and the minimum temperature display a positive correlation with the EOS, that is, the EOS exhibits a delaying trend with increasing temperature.

http://www.aloki.hu ● ISSN 1589 1623 (Print) ● ISSN 1785 0037 (Online)
DOI: http://dx.doi.org/10.15666/aeer/2303_47954826

Table 7. *Minimum distribution range of vegetation photosynthetic phenology changes due to driving factors*

Factors	SOS		EOS		LOS	
	Range	Mean (DOY)	Range	Mean (DOY)	Range	Mean (d)
Elevation	129~344m	144.59	79~191m	267.50	129~344m	123.00
Precipitation	361~435mm	137.00	435~509mm	267.25	361~435mm	132.90
Average temperature	3.20~4.50℃	136.19	-4.98~-2.64℃	258.03	-3.03~-1.09℃	127.43
Maximum temperature	7.82~9.61℃	136.45	4.33~5.98℃	258.15	2.44~6.80℃	127.99
Minimum temperature	-8.53~-6.36℃	134.15	-9.46~-7.44℃	257.35	-12.90~-6.91℃	126.11
Vegetation type	Cultivated vegetation	138.49	Alpine vegetation	262.99	Cultivated vegetation	133.74

When the elevation is below 344 m, the LOS displays a decreasing trend with increasing elevation, while when the elevation is above 344 m, the LOS manifests an increasing trend with increasing elevation. When the precipitation exceeds 435 mm, the LOS exhibits an extending trend with increasing precipitation. The average temperature, the maximum temperature and the minimum temperature are positively correlated with the LOS, that is, the LOS demonstrates an extending trend with increasing temperature.

Driver analysis on temporal variations

The Pearson correlation analysis method was used to analyze the relationships between SOS and precipitation, average temperature, maximum temperature and minimum temperature in the TNSFP region from 2001 to 2023, and the correlation coefficient distribution map was obtained (*Fig. 12*). From 2001 to 2023, the positive and negative correlations between SOS and precipitation, average temperature, maximum temperature and minimum temperature were relatively balanced, and the area with negative correlation between SOS and precipitation accounted for 54.55% of the total area of the study area, mainly concentrated in the northwest of Northeast Region and the west of North China Region, and the vegetation type was mainly coniferous forest; The positive correlation area accounts for 45.45% of the total area of the study area, which is mainly concentrated in the east of Inner Mongolia-Xinjiang Region, the south of Loess Plateau Region and the southeast of Northeast Region. The vegetation types are mainly grassland and broad-leaved forest. The areas with positive correlation between SOS and average temperature, maximum temperature and minimum temperature accounted for 56.28%, 56.86% and 54.21% of the total area of the study area, respectively. The regions with negative correlation between SOS and average temperature are mainly concentrated in the southeast and west of Northeast China and the northwest of Inner Mongolia-Xinjiang Region. The vegetation types are mainly grassland and herbosa. The regions with positive correlation are mainly concentrated in North China Region and the middle of the Loess Plateau Region. The vegetation types are mainly cultivated vegetation and shrub. The area with significant negative correlation between SOS and maximum temperature was mainly distributed in the southeast of Northeast China Region (P<0.05), and the vegetation type was mainly broad-leaved forest, that is, as the increase of maximum temperature, the SOS showed an advanced trend. The significant positive correlation between SOS and minimum temperature was mainly concentrated in North China Region

http://www.aloki.hu ● ISSN 1589 1623 (Print) ● ISSN 1785 0037 (Online)
DOI: http://dx.doi.org/10.15666/aeer/2303_47954826

(P<0.05), and the vegetation type was mainly shrub, that is, as the increase of minimum temperature, the SOS showed a delayed trend.

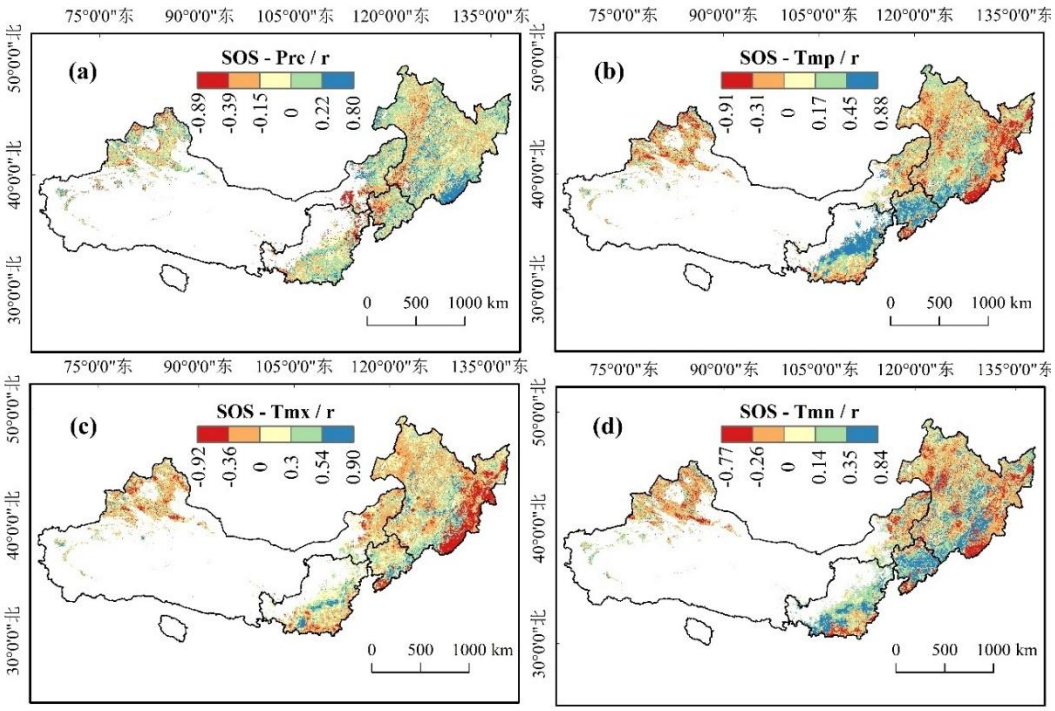

Figure 12. *Correlation coefficient distributions between SOS and climatic factors in the TNSFP region from 2001 to 2023*

The Pearson correlation analysis method was used to analyze the relationship between the EOS and precipitation, average temperature, maximum temperature, and minimum temperature in the TNSFP region from 2001 to 2023, and the distribution map of correlation coefficients was obtained (*Fig. 13*). From 2001 to 2023, the positive and negative correlation between EOS and precipitation was relatively balanced. The area with negative correlation between EOS and precipitation accounted for 57.93% of the total area of the study area. This area was mainly concentrated in the middle of Northeast China Region, North China Region, and the south of the Loess Plateau Region. The vegetation types were mainly coniferous forest and broad-leaved forest. The area with positive correlation accounted for 42.07% of the total area of the study area, mainly concentrated in the east of the Inner Mongolia-Xinjiang Region, and the vegetation type was mainly grassland. The average correlation coefficients between EOS and average temperature, maximum temperature, and minimum temperature were 0.121, 0.111, and 0.103, respectively. Overall, positive correlations dominated, which means that the EOS shows a delayed trend with the increase of temperature. The positive correlation regions accounted for 65.07%, 65.53%, and 65.68% of the total area of the study area, respectively. The EOS of vegetation in North China Region and the middle of the Loess Plateau Region showed a significant positive correlation with the average temperature (P<0.05), and the vegetation types were mainly cultivated vegetation and shrubs. The regional distribution of positive correlation between EOS and maximum temperature and minimum temperature was scattered.

http://www.aloki.hu ● ISSN 1589 1623 (Print) ● ISSN 1785 0037 (Online)
DOI: http://dx.doi.org/10.15666/aeer/2303_47954826

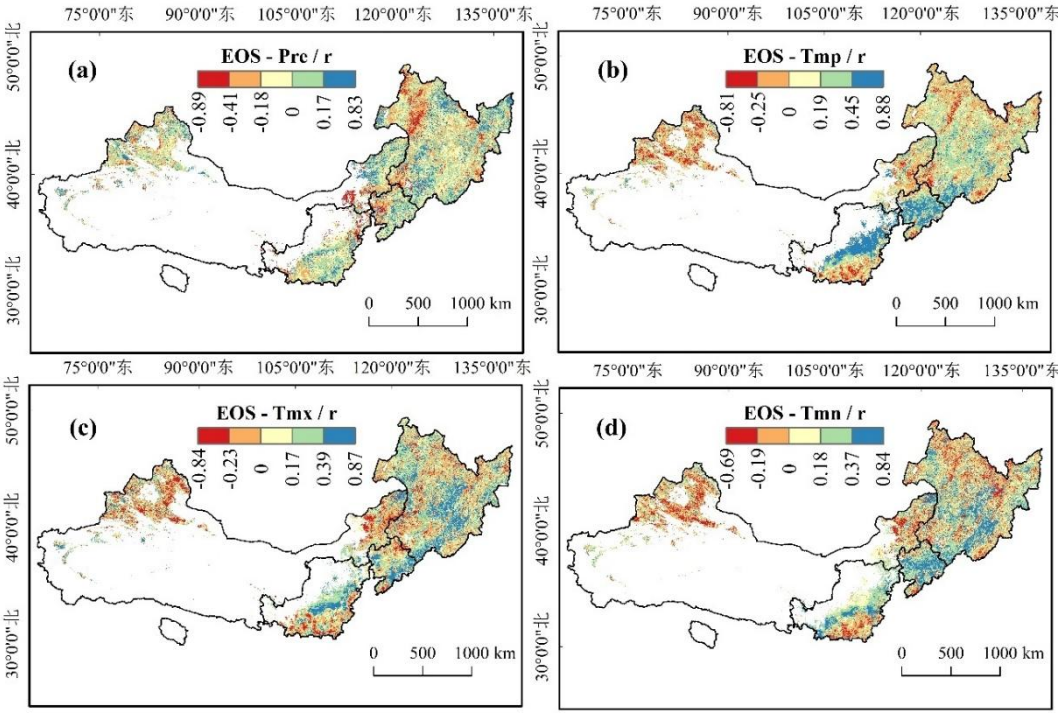

Figure 13. *Correlation coefficient distributions between EOS and climatic factors in the TNSFP region from 2001 to 2023*

The Pearson correlation analysis method was used to analyze the relationships between the LOS, precipitation, average temperature, maximum temperature, and minimum temperature in the TNSFP region from 2001 to 2023. A distribution map of the correlation coefficients was obtained (*Fig. 14*). From 2001 to 2023, the positive and negative correlations between the LOS and precipitation were relatively balanced. The areas with a positive correlation between the LOS and precipitation accounted for 54.78% of the total study area and were mainly concentrated in the southern part of Northeast China Region, North China Region, and the middle of the Loess Plateau Region. The predominant vegetation types in these areas were grasslands and cultivated plants. In contrast, the areas with a negative correlation accounted for 45.22% of the total study area and were scattered across parts of the Northeast China Region. The vegetation mainly consisted of broad-leaved forests and coniferous forests. The average correlation coefficients between the LOS and average temperature, maximum temperature, and minimum temperature were 0.084, 0.079, and 0.068, respectively, indicating a weak positive correlation. That is, as the temperature increased, the LOS showed a weak tendency to extend. The regions with positive correlations accounted for 61.58%, 64.82%, and 59.47% of the total study area, respectively. There was a significant positive correlation between the LOS and the maximum temperature in the southeast of Northeast China Region ($P<0.05$). This implies that an increase in temperature would lead to an extension of the LOS in this area, where the vegetation is predominantly broad-leaved forest.

http://www.aloki.hu ● ISSN 1589 1623 (Print) ● ISSN 1785 0037 (Online)
DOI: http://dx.doi.org/10.15666/aeer/2303_47954826

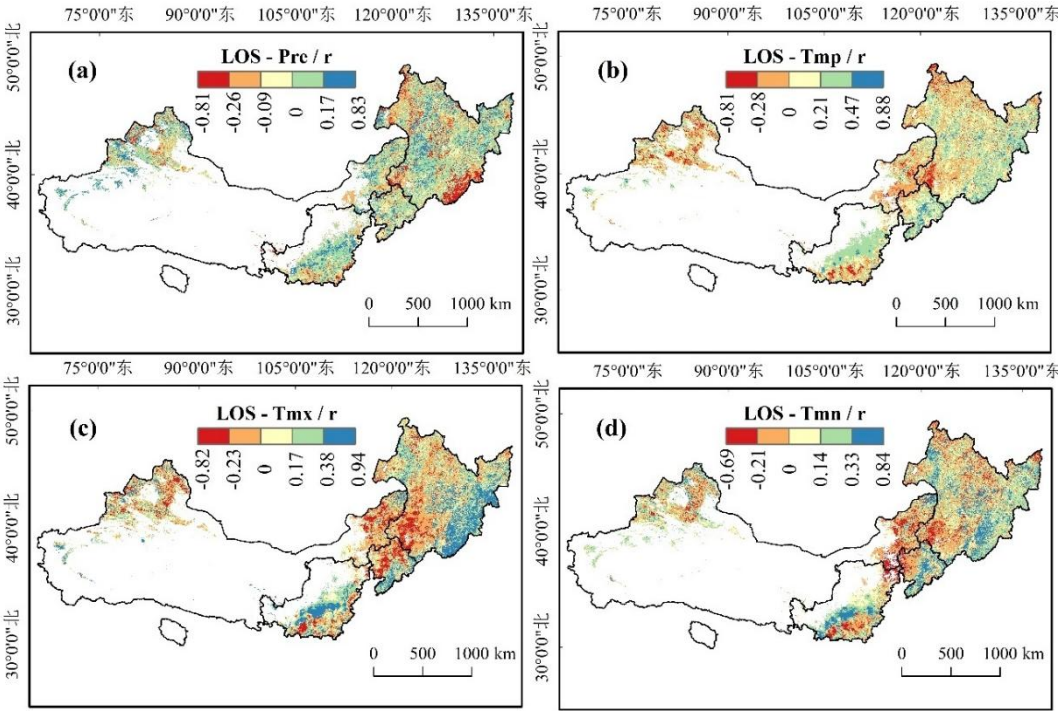

Figure 14. *Correlation coefficient distributions between LOS and climatic factors in the TNSFP region from 2001 to 2023*

Discussion

Changes in vegetation photosynthetic phenology

From 2001 to 2023, the average SOS in the TNSFP region was primarily concentrated between 105 and 150 DOY, the EOS was mainly concentrated between 250 and 290 DOY, and the LOS was primarily concentrated between 105 and 185 days. These results are broadly consistent with the distribution range of vegetation photosynthetic phenology in northern China described by Zhao (2022), Zhang (2023), and Liu et al. (2024). The spatial distribution of the SOS, EOS, and LOS in the western and southern parts of the study area exhibits characteristics of early-late-long, while the eastern and northern parts display late-early-short characteristics. The vegetation photosynthetic phenology in the study area demonstrates strong spatial heterogeneity, which may be related to geographical location, hydrothermal conditions, etc. Different latitudes and elevation have varying distribution ranges of climate factors, and the region features different vegetation types, resulting in significant differences in the start, end, and duration of the growing season.

In the context of global warming, exploring the trends in vegetation photosynthetic phenology plays a crucial role in understanding the impact of global warming on terrestrial ecosystems. Xue (2024) analyzed the trends in vegetation photosynthetic phenology in China based on SIF data, finding that the SOS generally shows an advancing trend, the EOS shows a delaying trend, and the LOS shows an extending trend. Related studies also indicate that in high-latitude regions of the north, the SOS shows an advancing trend, the EOS shows a delaying trend, and the trend of the EOS is faster than that of the SOS (Walther et al., 2002; Jeganathan et al., 2014). This study found that from 2001 to 2023, the TNSFP region showed an advancing trend in the SOS (0.16 d/a), a

http://www.aloki.hu ● ISSN 1589 1623 (Print) ● ISSN 1785 0037 (Online)
DOI: http://dx.doi.org/10.15666/aeer/2303_47954826

delaying trend in the EOS (0.20 d/a), and an extending trend in the LOS (0.26 d/a). This is consistent with the research results of Cong et al. (2022) and Zhou et al. (2024), although there are slight differences in the rates of change, which may be due to differences in data sources, research periods, and study areas (Wang et al., 2022). Additionally, changes in vegetation photosynthetic phenology are closely related to the external environment, with good hydrothermal conditions and sufficient nutrients being key to vegetation growth and development. Therefore, accurately identifying the key regulatory factors affecting vegetation phenology in the study area is helpful for a deeper understanding of the response mechanisms and coping strategies of terrestrial ecosystems in northern China under global warming conditions.

Responses of vegetation photosynthetic phenology to driving factors

The principal driving factors influencing vegetation photosynthetic phenology encompass both natural factors and socio-economic factors. Climatic factors play a dominant role in affecting the variations of vegetation photosynthetic phenology within the study area, with temperature and precipitation being the crucial driving factors that result in the changes of vegetation photosynthetic phenology (Liu et al., 2022). Relevant studies have demonstrated that the growth of vegetation in terrestrial ecosystems is most significantly impacted by climatic factors. Specifically, vegetation photosynthetic phenology is primarily regulated by temperature and precipitation. Moreover, in arid and semi-arid regions, the sensitivity of vegetation photosynthetic phenology to precipitation is greater than that to temperature (Zhou et al., 2023), which coincides with the conclusion of the present study. The evident spatial heterogeneity of vegetation photosynthetic phenology in the TNSFP region might stem from the uneven spatial distribution of water and heat conditions in the study area.

In the results of single-factor detection, precipitation stands out as the most significant driving factor explaining the spatial differences in the SOS and LOS. This is likely due to its pronounced spatial heterogeneity in distribution. Studies indicate that in arid and semi-arid regions, the SOS and LOS are more significantly influenced by precipitation. This could be attributed to the limited availability of water around vegetation, which restricts its growth and leads to an earlier trend in the SOS (Zhang et al., 2022). Additionally, precipitation in these regions is primarily concentrated in summer, accompanied by high evaporation. An increase in precipitation can effectively alleviate water stress on vegetation, altering soil moisture conditions. When soil moisture reaches a certain threshold, it may promote the early commencement of the plant growth season. However, if the increase in precipitation is outweighed by evaporation, it may result in an inability of soil moisture to sustain plant growth continuously, leading to a lag in the SOS. In the study area, the EOS is more significantly influenced by minimum temperature, followed by maximum temperature. An increase in minimum temperature may lead to a warmer autumn, fewer frost days, and a delayed first frost, resulting in a delayed trend in the EOS (Ren et al., 2021). Simultaneously, an increase in precipitation may lead to a decrease in average maximum temperature, resulting in an earlier trend in the EOS, primarily concentrated in the Great Khingan Mountains Area in the northeastern part of the study area. Although slope orientation and slope have a minor explanatory power for vegetation phenology, climate change is largely attributed to topographic factors and latitude differences, playing a significant role in the balance of the entire ecosystem.

http://www.aloki.hu ● ISSN 1589 1623 (Print) ● ISSN 1785 0037 (Online)
DOI: http://dx.doi.org/10.15666/aeer/2303_47954826

Vegetation photosynthetic phenology is a complex dynamic process. A single factor cannot fully explain the heterogeneity of vegetation photosynthetic phenology in space. Instead, complex interactions among multiple factors should be considered. The interaction between various driving factors can have a more significant impact on the changes in vegetation photosynthetic phenology (Kong et al., 2017). Relevant studies have shown that the interaction between monthly average temperature and precipitation can more effectively explain the changes in vegetation photosynthetic phenology in the Qilian Mountains than a single factor (Li et al., 2022). This is consistent with the conclusion of this study that the interaction between precipitation and average temperature has the strongest explanatory power for the changes in the SOS and LOS in the study area. The interaction between precipitation and minimum temperature has the strongest explanatory power for the EOS, which is consistent with the research conclusion of Yao (2022), who found that the sensitivity of average minimum temperature to the EOS in Northwest China gradually increases with increasing precipitation and exhibits a phased pattern. This study also found that the interaction between vegetation types and socioeconomic factors with climate factors exhibits strong explanatory power. This may be because there are significant differences between different vegetation types, each with its unique physiological characteristics, sensitivity to climate, and access to different resources in a limited environment, which is influenced by environmental heterogeneity (Zhao et al., 2024). At the same time, socioeconomic factors indicate human activities, and the intensity of human activities can indirectly affect the growth and development process of vegetation by influencing the underlying surface of vegetation growth (Yuan et al., 2023).

Uncertainty analysis

This study extracts phenological information from the TNSFP region based on GOSIF products. Multiple studies have demonstrated the reliability of using SIF data to monitor actual photosynthesis in vegetation (Meroni et al., 2009; Liu et al., 2018; Li and Xiao, 2019), and a strong linear relationship exists between SIF and GPP (Frankenberg et al., 2011; Guanter et al., 2012). Hence, extracting vegetation photosynthetic phenological parameters using SIF data is feasible. However, the low spatial resolution of GOSIF products (0.05°) may somewhat affect the accuracy of phenological extraction. Existing research has indicated that SIF exhibits high sensitivity to the environment, offering significant potential for monitoring vegetation photosynthetic phenology (Qiu et al., 2022). In future research, the selection of higher-resolution long-term time series data, combined with additional driving factors (such as solar radiation, wind speed, soil moisture, etc.), could enhance the accuracy of reflecting the spatiotemporal variation characteristics of vegetation photosynthetic phenology in the TNSFP region and its response to driving factors.

Conclusion

From 2001 to 2023, the average SOS values of vegetation in the Three-North Shelter Forest Program region were primarily concentrated within the range of 105 to 150 DOY, exhibiting an overall trend of advancement, with an advancement rate of 0.16 d/a; the average EOS values were primarily concentrated within the range of 250 to 290 DOY, indicating an overall trend of delay, with a delay rate of 0.20 d/a; the average LOS values were primarily concentrated within the range of 105 to 185 days, exhibiting an overall

http://www.aloki.hu ● ISSN 1589 1623 (Print) ● ISSN 1785 0037 (Online)
DOI: http://dx.doi.org/10.15666/aeer/2303_47954826

trend of extension, with an extension rate of 0.26 d/a. Significant differences exist in vegetation photosynthetic phenology among various vegetation types within the Three-North Shelter Forest Program region. In interannual variations, with the exception of herbosa, alpine vegetation, and broad-leaved forest, the SOS of other vegetation types exhibits an advancing trend, with shrub showing the most pronounced advancement; whereas, except for herbosa and coniferous forest, the EOS of other vegetation types demonstrates a significant delay. The LOS of cultivated vegetation, shrub, and broad-leaved forest is extending, while for other vegetation types it is shortening, with herbosa exhibiting the most pronounced shortening. Overall, the SOS and EOS in the study area exhibit low fluctuation, while the LOS experiences both low fluctuation and relatively low fluctuation, with the latter predominantly occurring in the Northeastern Region. From the perspective of future trends, the SOS in most parts of the study area is expected to delay, the EOS to advance, and the LOS to shorten. In terms of spatial heterogeneity, precipitation stands out as the most influential factor for both SOS and LOS, whereas minimum temperature is the most significant factor for EOS. Notably, the interaction between these two factors surpasses the individual impact of either on vegetation photosynthetic phenology, highlighting the substantial influence of precipitation and temperature on the phenology of vegetation in the study area. In terms of temporal variation, the correlations between vegetation phenology and temperature and precipitation showed obvious spatial differences. The impact of temperature on vegetation phenology is more pronounced, mainly showing a positive effect. Therefore, the combined effects of natural and social factors have a more prominent impact on the vegetation photosynthetic phenology in the study area.

Acknowledgements. This work is supported by the Key Research and Development Plan of Inner Mongolia, China (2023YFDZ0026), National Natural Science Foundation of China (32260389), Natural Science Foundation of Inner Mongolia, China (2024QN03077) and Research Team Construction Project of Forestry College, Inner Mongolia Agricultural University, China.

REFERENCES

[1] An, N., Ning, X. L., Hai, Q. S., Ding, L. (2020): Optical model for estimating the spatial and temporal distribution of vegetation net primary productivity in Hunshandake Sandyland in recent 15 years. – Journal of Arid Land Resources and Environment 34(4): 168-175.

[2] Anniwaer, N., Li, X. Y., Wang, K., Xu, H., Hong, S. B. (2024): Shifts in the trends of vegetation greenness and photosynthesis in different parts of Tibetan Plateau over the past two decades. – Agricultural and Forest Meteorology 345: 109851.

[3] Cao, J. H. (1988): The analysis on the significant testing ways of the simple linear regression. – Journal of Xi'an Polytechnic University Z1: 78-82.

[4] Cao, P. Y., Zhang, L. M., Li, S. G., Zhang, J. H. (2016): Review on vegetation phenology observation and phenological index extraction. – Advances in Earth Science 31(4): 365-376.

[5] Cao, S. X., Liu, G. C., Ma, H. (2017): Dynamic analysis of vegetation change in north China. – Acta Ecologica Sinica 37(15): 5023-5030.

[6] Caparros-Santiago, J. A., Rodriguez-Galiano, V., Dash, J. (2021): Land surface phenology as indicator of global terrestrial ecosystem dynamics: A systematic review. – ISPRS Journal of Photogrammetry and Remote Sensing 171: 330-347.

http://www.aloki.hu ● ISSN 1589 1623 (Print) ● ISSN 1785 0037 (Online)
DOI: http://dx.doi.org/10.15666/aeer/2303_47954826

[7] Churkina, G., Schimel, D., Braswell, B. H., Xiao, X. (2005): Spatial analysis of growing season length control over net ecosystem exchange. – Global Change Biology 11(10): 1777-1787.
[8] Cleland, E. E., Allen, J. M., Crimmins, T. M., Dunne, J. A., Pau, S., Travers, S. E., Zavaleta, E. S., Wolkovich, E. M. (2012): Phenological tracking enables positive species responses to climate change. – Ecology 93(8): 1765-1771.
[9] Cong, N., Zhang, Y., Zhu, J. (2022): Temperature sensitivity of vegetation phenology in spring in mid- to high-latitude regions of Northern Hemisphere during the recent three decades. – Chinese Journal of Plant Ecology 46(2): 125.
[10] Dao, R. N. (2019): Effects of Climate and Land Use Change on Vegetation NDVI in the Three North Region. – Hohhot: Inner Mongolia Normal University.
[11] Fensholt, R., Proud, S. R. (2012): Evaluation of Earth Observation based global long term vegetation trends-Comparing GIMMS and MODIS global NDVI time series. – Remote Sensing of Environment 119: 131-147.
[12] Frankenberg, C., Fisher, J. B., Worden, J., Badgley, G., Saatchi, S. S., Lee, J-E., Toon, G. C., Butz, A., Jung, M., Kuze, A., Yokota, T. (2011): New global observations of the terrestrial carbon cycle from GOSAT: Patterns of plant fluorescence with gross primary productivity. – Geophysical Research Letters 38(17).
[13] Frankenberg, C., O'Dell, C., Berry, J., Guanter, L., Joiner, J., Köhler, P., Pollock, R., Taylor, T. E. (2014): Prospects for chlorophyll fluorescence remote sensing from the Orbiting Carbon Observatory-2. – Remote Sensing of Environment 147: 1-12.
[14] Fu, Y. Y., Zhao, J. J., Zhang, H. Y., He, H. S., Guo, X. Y. (2016): Spatiotemporal variation of vegetation phenology in the Daxing'an Mountains stratified byeco-geographical regions. – Chinese Journal of Applied Ecology 27(09): 2797-2806.
[15] Guanter, L., Frankenberg, C., Dudhia, A., Lewis, P. E., Gómez-Dans, J., Kuze, A., Suto, H., Grainger, R. G. (2012): Retrieval and global assessment of terrestrial chlorophyll fluorescence from GOSAT space measurements. – Remote Sensing of Environment 121: 236-251.
[16] Guanter, L., Zhang, Y., Jung, M., Joiner, J., Voigt, M., Berry, J. A., Frankenberg, C., Huete, A. R., Zerco-Tejada, P., Lee, J., Moran, M. S., Ponce-Campos, G., Beer, C., Camps-Valls, G., Buchmann, N., Giamelle, D., Klumpp, K., Cescatti, A., Baker, J. M., Griffis, T. J. (2014): Global and time-resolved monitoring of crop photosynthesis with chlorophyll fluorescence. – Proceedings of the National Academy of Sciences 111(14): E1327-E1333.
[17] Guanter, L., Aben, I., Tol, P., Krijger, J. M., Hollstein, A., Köhler, P., Damm, A., Joiner, J., Frankenberg, C., Landgraf, J. (2015): Potential of the TROPO spheric Monitoring Instrument (TROPOMI) onboard the sentinel-5 precursor for the monitoring of terrestrial chlorophyll fluorescence. – Atmospheric Measurement Techniques 8(3): 1337-1352.
[18] Huang, L., Cao, W., Gong, G. L., Zhao, G. S. (2016): Spatial and temporal variations in ecosystems in the three northern regions of China, 2000-2010. – Acta Ecologica Sinica 36(1): 107-117.
[19] Jeganathan, C., Dash, J., Atkinson, P. M. (2014): Remotely sensed trends in the phenology of northern high latitude terrestrial vegetation, controlling for land cover change and vegetation type. – Remote Sensing of Environment 143: 154-170.
[20] Jeong, S. J., Schimel, D., Frankenberg, C., Drewry, D. T., Fisher, J. B., Verma, M., Berry, J. A., Lee, J., Joiner, J. (2017): Application of satellite solar-induced chlorophyll fluorescence to understanding large-scale variations in vegetation phenology and function over northern high latitude forests. – Remote Sensing of Environment 190(1): 178-187.
[21] Joiner, J., Guanter, L., Lindstrot, R., Voigt, M., Vasilkov, A. P., Middleton, E. M., Huemmrich, K. F., Yoshida, Y., Frankenberg, C. (2013): Global monitoring of terrestrial chlorophyll fluorescence from moderate-spectral-resolution near-infrared satellite measurements: methodology, simulations, and application to GOME-2. – Atmospheric Measurement Techniques 6(10): 2803-2823.

http://www.aloki.hu ● ISSN 1589 1623 (Print) ● ISSN 1785 0037 (Online)
DOI: http://dx.doi.org/10.15666/aeer/2303_47954826

[22] Joiner, J., Yoshida, Y., Vasilkov, A. P., Schaefer, K., Jung, M., Guanter, L., Zhang, Y., Garrity, S., Middleton, E. M., Huemmrich, K. F., Gu, L., Belelli Marchesini, L. (2014): The seasonal cycle of satellite chlorophyll fluorescence observations and its relationship to vegetation phenology and ecosystem atmosphere carbon exchange. – Remote Sensing of Environment 152: 375-391.
[23] Karkauskaite, P., Tagesson, T., Fensholt, R. (2017): Evaluation of the plant phenology index (PPI), NDVI and EVI for start-of-season trend analysis of the Northern Hemisphere boreal zone. – Remote Sensing 9(5): 485.
[24] Kong, D. D., Zhang, Q., Huang, W. L., Gu, X. H. (2017): Vegetation phenology change in Tibetan Plateau from 1982 to 2013 and its related meteorological factors. – Acta Geographica Sinica 72(01): 39-52.
[25] Kross, A. S., Roulet, N. T., Moore, T. R., Lafleur, P. M., Humphreys, E. R., Seaquist, J. W., Flanagan, L. B., Aurela, M. (2014): Phenology and its role in carbon dioxide exchange processes in northern peatlands. – Journal of Geophysical Research: Biogeosciences 119(7): 1370-1384.
[26] Li, X., Xiao, J. (2019): A global, 0.05-degree product of solar-induced chlorophyll fluorescence derived from OCO-2, MODIS, and reanalysis data. – Remote Sensing 11(5): 517.
[27] Li, Y., Zhang, C. C., Luo, W. R., Gao, W. J. (2019): Summer maize phenology monitoring based on normalized difference vegetation index reconstructed with improved maximum value composite. – Transactions of the Chinese Society of Agricultural Engineering 35(14): 159-165.
[28] Li, C., Zou, Y. Y., He, J. F., Zhang, W., Gao, L. L., Zhuang, D. F. (2022): Response of vegetation phenology to the interaction of temperature and precipitation changes in Qilian mountains. – Remote Sensing 14(5): 1248.
[29] Lin, N., Xu, L., Lu, F. Q., Wang, S. C., Wang, M., Li, Q. Y. (2023): Simulation of spring phenology of Salicaceae trees in North China. – Acta Ecologica Sinica 43(6): 1-13.
[30] Liu, L., Yang, X., Zhou, H., Liu, S. S., Zhou, L., Li, X. H., Yang, J. H., Han, X. Y., Wu, J. J. (2018): Evaluating the utility of solar-induced chlorophyll fluorescence for drought monitoring by comparison with NDVI derived from wheat canopy. – Science of the Total Environment 625: 1208-1217.
[31] Liu, X. T., Zhou, L., Shi, H., Wang, S. Q., Chi, Y. G. (2018): Phenological characteristics of temperate coniferous and broad-leaved mixed forests based on multiple remote sensing vegetation indices, chlorophyll fluorescence and CO_2 flux data. – Acta Ecologica Sinica 38(10): 3482-3494.
[32] Liu, Y., Zhou, W., Gao, S., Ma, X. L., Yan. K. (2022): Phenological responses to snow seasonality in the qilian mountains is a function of both elevation and vegetation types. – Remote Sensing 14(15): 3629.
[33] Liu, B., Luo, W. H., Feng, D. E., Li, C. (2024): Responses of Vegetation Photosynthetic Phenology in Spring to Climate Factors in Northern China. – Research of Soil and Water Conservation 31(06): 237-242.
[34] Meroni, M., Rossini, M., Guanter, L., Alonso, L., Rascher, U., Colombo, R., Moreno, J. (2009): Remote sensing of solar-induced chlorophyll fluorescence: Review of methods and applications. – Remote Sensing of Environment 113(10): 2037-2051.
[35] Pettorelli, N., Vik, J. O., Mysterud, A., Gaillard, J., Tucher, C. J., Stenseth, N. C. (2005): Using the satellite-derived NDVI to assess ecological responses to environmental change. – Trends in Ecology & Evolution 20(9): 503-510.
[36] Piao, S., Liu, Q., Chen, A., Janssens, A., Fu, Y., Dai, J., Liu, L., Lian, X., Shen, M., Zhu, X. (2019): Plant phenology and global climate change: Current progresses and challenges. – Global Change Biology 25(6): 1922-1940.
[37] Qiu, P. H., Xia, Z. M., You L. (2020): Process monitoring ROC curve for evaluating dynamic screening methods. – Technometrics 62(2): 236-248.

http://www.aloki.hu ● ISSN 1589 1623 (Print) ● ISSN 1785 0037 (Online)
DOI: http://dx.doi.org/10.15666/aeer/2303_47954826

[38] Qiu, R., Li, X., Han, G., Xiao, J., Ma, X., Gong, W. (2022): Monitoring drought impacts on crop productivity of the US Midwest with solar-induced fluorescence: GOSIF outperforms GOME-2 SIF and MODIS NDVI, EVI, and NIRv. – Agricultural and Forest Meteorology 323: 109038.
[39] Ren, P., Liu, Z., Zhou, X., Peng, C., Xiao, J., Wang, S., Li, X., Li, P. (2021): Strong controls of daily minimum temperature on the autumn photosynthetic phenology of subtropical vegetation in China. – Forest Ecosystems 8: 1-12.
[40] Sa, R., Hua, Y., Zhai, K., Wang, T., Zhang, H. (2023): Assessing ecological services in the Three-North Shelter Forest Area of China using remote sensing. – Applied Ecology & Environmental Research 21(1): 261-285.
[41] Sen, P. K. (1968): Estimates of the regression coefficient based on Kendall's tau. – Journal of the American statistical association 63(324): 1379-1389.
[42] Sun, Y., Frankenberg, C., Wood, J. D., Schimel, D. S., Jung, M., Guanter, L., Drewry, D. T., Verma, M., Porcar-Castell, A., Criffis, T. J., Gu, L., Magney, T. S., Köhler, P., Evans, B., Yuen, K. (2017): OCO-2 advances photosynthesis observation from space via solar-induced chlorophyll fluorescence. – Science 358(6360): eaam5747.
[43] Walther, G. R., Post, E., Convey, P., Menzel, A., Parmesan, C., Beebee, T. J. C., Fromentin, J. M., Hoegh-Guldberg, O., Bailein, F. (2002): Ecological responses to recent climate change. – Nature 416(6879): 389-395.
[44] Wang, Q., Zhang, B., Dai, S. P., Zhang, F. F., Zhao, Y. F., Yin, H. X., He, X. Q. (2012): Analysis of the vegetation cover change and its relationship with factors in the Three-North Shelter Forest Program. – China Environmental Science 32(7): 1302-1308.
[45] Wang, J. F., Xu, C. D. (2017): Geodetector: Principle and prospective. – Acta Geographica Sinica 72(01): 116-134.
[46] Wang, L., Dong, L., Hu, T. Y., Guo, K. (2021): History and prospect of vegetation map compilation in China. – Scientia Sinica (Vitae) 51(03): 219-228.
[47] Wang, C., Wu, Y., Hu, Q., Hu, J., Chen, Y., Lin, S., Xie, Q. (2022): Comparison of vegetation phenology derived from solar-induced chlorophyll fluorescence and enhanced vegetation index, and their relationship with climatic limitations. – Remote Sensing 14(13): 3018.
[48] Xia, A. Q., Wang, Y. F., Hao, Y. B., Hu, R. H., Wang, F., Wu, W. C., Cui, X. Y. (2020): Research progress on estimation of vegetation carbon storage of grasslands on complex terrain by remote sensing technology. – Acta Ecologica Sinica 40(18): 6338-6350.
[49] Xiao, J. F., Zhuang, Q. L., Baldocchi, D. D., Law, B. E., Richardson, A. D., Chen, J. Q., Oren, R., Starr, G., Noormets, A., Ma, S. Y., Verma, S. B., Wharton, S., Wofsy, S. C., Bolstad, P. V., Burns, S. P., Cook, D. R., Curtis, P. S., Drake, B. G., Falk, M., Fischer, M. L., Foster, D. R., Gu, L. H., Hadley, J. L., Hollinger, D. Y., Katul, G. G., Litvak, M., Martin, T. A., Matamala, R., Mcnulty, S., Meyers, T. P., Monson, R. K., Munger, J. W., Oechel, W. C., Paw, U. K. T., Schmid, H. P., Scott, R. L., Sun, G., Suyker, A. E., Torn, M. S. (2008): Estimation of net ecosystem carbon exchange for the conterminous United States by combining MODIS and AmeriFlux data. – Agricultural and Forest Meteorology 148(11): 1827-1847.
[50] Xie, S. D., Mo, X. G., Hu, S., Chen, X. J. (2020): Responses of vegetation greenness to temperature and precipitation in the Three-North Shelter Forest Program. – Geographical Research 39(01): 152-165.
[51] Xu, R., Huang, X. J., Wang, P. Y., Liu, Z. M., Liang, J., Yang, L., Zhang, X. Y. (2022): Teritoral spatial carbon neurality reaizaton degree of the Yellow River Basin: hcase study of the Inner Mongolia section. – Acta Ecologica Sinica 42(23): 9651-9662.
[52] Xue, Y. Y. (2024): Response of photosynthetic phenology of vegetation to temperature-precipitation-drought in China. – Guizhou Normal University.
[53] Yang, X., Guo, R., Knops, J. M. H., Mei, L., Kang, F., Zhang, T., Guo, J. (2020): Shifts in plant phenology induced by environmental changes are small relative to annual phenological variation. – Agricultural and Forest Meteorology 294: 108144.

http://www.aloki.hu ● ISSN 1589 1623 (Print) ● ISSN 1785 0037 (Online)
DOI: http://dx.doi.org/10.15666/aeer/2303_47954826

[54] Yao, R. P. (2022): Vegetation Phenological Variation and Its Response to Climate Changes in Northwest China. – Northwest Normal University.
[55] Yoshida, Y., Joiner, J., Tucker, C., Berry, J., Lee, J. E., Walker, G., Beichle, R., Koster, R., Lyapustin, A., Wang, Y. (2015): The 2010 Russian drought impact on satellite measurements of solar-induced chlorophyll fluorescence: Insights from modeling and comparisons with parameters derived from satellite reflectances. – Remote Sensing of Environment 166: 163-177.
[56] Yu, H. Y., Luedeling, E., Xu, J. C. (2010): Winter and spring warming result in delayed spring phenology on the Tibetan Plateau. – Proceedings of the National Academy of Sciences 107(51): 22151-22156.
[57] Yuan, Z. H., Sa, C. L., Yin, S. (2021): Research on vegetation phenological changes in the Otindag sandy land Based on MODIS NDVI and EVI. – China Environmental Science 41(11): 5254-5263.
[58] Yuan, H. H., Yan, J. B., Zhang, J. L., Wang, Z., Xu, W. G., Zhang, H. N. (2023): Influences of climate change and human activities on vegetation phenology of Shanghai. – Acta Ecologica Sinica 43(21): 8803-8815.
[59] Zarco-Tejada, P. J., Berni, J. A., Suárez, L., Sepulcre-Cantó, G., Morales, F., Miller, J. R. (2009): Imaging chlorophyll fluorescence with an airborne narrow-band multispectral camera for vegetation stress detection. – Remote Sensing of Environment 113(6): 1262-1275.
[60] Zhang, Y., Guanter, L., Berry, J. A., van der Tol, C., Yang, X., Tang, J., Zhang, F. (2016): Model-based analysis of the relationship between sun-induced chlorophyll fluorescence and gross primary production for remote sensing applications. – Remote Sensing of Environment 187: 145-155.
[61] Zhang, J. R., Tong, X. J., Meng, P., Zhang, J. S., Liu, P. R. (2020): Comparative study on phenology in a mountainous plantation in northern China based on vegetation index, chlorophyll fluorescence and carbon flux. – Journal of Beijing Forestry University 42(11): 17-26.
[62] Zhang, Q., Chen, W. (2021): Ecosystem water use efficiency in the Three-North Region of China based on long-term satellite data. – Sustainability 13(14): 7977.
[63] Zhang, R., Qi, J., Leng, S., Wang, Q. (2022): Long-term vegetation phenology changes and responses to preseason temperature and precipitation in Northern China. – Remote Sensing 14(6): 1396.
[64] Zhang, X. T. (2023): Research on spring phenology and its sensitivity to climate in boreal forests. – Northeast Normal University.
[65] Zhang, J., Zhang, Y. (2024): Quantitative Assessment of the Impact of the Three-North Shelter Forest Program on Vegetation Net Primary Productivity over the Past Two Decades and Its Environmental Benefits in China. – Sustainability 16(9): 3656.
[66] Zhao, X. Y., Luo, L., Wang, Y. R., Zhang, Q., Liu, Y. F. (2014): Extreme Temperature Events in Eastern Edge of the Qinghai-Tibet Plateau from 1963 to 2012. – Resources Science 36(10): 2113-2122.
[67] Zhao, L. R. (2022): The response of vegetation phenology to climate change in northern China from 2001 to 2020. – Inner Mongolia Normal University.
[68] Zhao, Z. H., Wang, X. Y., Li, R. J., Luo, W., Wu, C. Y. (2023): Impacts of climate extremes on autumn phenology in contrasting temperate and alpine grasslands in China. – Agricultural and Forest Meteorology 336: 109495.
[69] Zhao, X. R., Liu, J., Yang, S. K., Zhang, Q., Gao, F., Liu, Y. L. (2023): Spatio-temporal variations of typical woodland and grassland phenology and its response to meteorological factors in Northern China. – Acta Ecologica Sinica 43(9): 3744-3755.
[70] Zhao, Y. P., Liu, J. F., Wang, Q., Huang, R. Z., Sun, J. Y., Nie, W., Yang, S. W. (2024): Differences in the response of different vegetation types to frost event and their driving forces. – Acta Ecologica Sinica 44(15): 6744-6757.

http://www.aloki.hu ● ISSN 1589 1623 (Print) ● ISSN 1785 0037 (Online)
DOI: http://dx.doi.org/10.15666/aeer/2303_47954826

[71] Zheng, X., Zhu, J. J., Yan, Y. (2013): Estimation of farmland shelterbelt area in the Three-North Shelter / Protective Forest Program regions of China based on multi-scale remote sensing data. – Chinese Journal of Ecology 32(05): 1355-1363.
[72] Zhou, D., Zhao, S., Zhang, L., Liu, S. (2016): Remotely sensed assessment of urbanization effects on vegetation phenology in China's 32 major cities. – Remote Sensing of Environment 176: 272-281.
[73] Zhou, W., Chi, Y. G., Zhou, L. (2021): Vegetation phenology in the Northern Hemisphere based on the solar-induced chlorophyll fluorescence. – Journal of Plant Ecology 45(4): 345-354.
[74] Zhou, H. R., Sun, H., Shi, Z. W., Peng, F., Lin, Y. (2023): Solar-Induced Chlorophyll Fluorescence data-based study on the spatial and temporal patterns of vegetation phenology in the Northern Hemisphere during the period of 2007-2018. – National Remote Sensing Bulletin 27(02): 376-393.
[75] Zhou, Y. K., Zhang, R. X., Sun, W. B., Zhang, S. H. (2024): Spatiotemporal Characteristics of vegetation Phenology in Northeast China based on Solar-induced Chlorophyll Fluorescence and Response to Climate. – Remote Sensing Technology and Application 39(1): 185-197.

http://www.aloki.hu ● ISSN 1589 1623 (Print) ● ISSN 1785 0037 (Online)
DOI: http://dx.doi.org/10.15666/aeer/2303_47954826